AD-A034 947 AIR FORCE INST OF TECH WRIGHT-PATTERSON AFB OHIO SCH--ETC F/G 22/2
MAXIMUM PAYLOAD ORBITAL TRANSFERS FOR A SPACE SHUTTLE SOLID-FUE--ETC(U)
DEC 76 J W MOCKO

UNCLASSIFIED GA/MC/76D-11 NL

1 OF 2
ADA034947

UNITED STATES AIR FORCE

AIR UNIVERSITY

AIR FORCE INSTITUTE OF TECHNOLOGY

Wright-Patterson Air Force Base, Ohio

GA/MC/76D-11

MAXIMUM PAYLOAD ORBITAL TRANSFERS FOR A SPACE SHUTTLE SOLID-FUEL UPPER STAGE VEHICLE

THESIS

GA/MC/76D-11

John W. Mocko
1st Lt USAF

Approved for public release; distribution unlimited

(14) GA/MC/76D-11

(6) MAXIMUM PAYLOAD ORBITAL TRANSFERS FOR A SPACE SHUTTLE SOLID-FUEL UPPER STAGE VEHICLE.

THESIS (9) Master's thesis

Presented to the Faculty of the School of Engineering

of the Air Force Institute of Technology

Air University

in Partial Fulfillment of the

Requirements for the Degree of

Master of Science

(12) 112p.

(11) Dec 76

by

(10) John W. Mocko, B.S.

1st Lt USAF

Graduate Astronautics

Preface

This thesis is an investigation of the present capabilities of a specific Space Shuttle Upper Stage Vehicle. It is also an attempt to make a contribution towards the economical use of the vehicle in terms of various types of energy management. The approach to the problem is general in nature so that it may be extended to a wide range of shuttle missions and vehicles.

I would like to acknowledge those who have helped and supported me throughout this project. My thanks go to my advisor, Professor Gerald M. Anderson, for his aid, especially in the initial phase of the study. I am also indebted to Dr. Richard M. Potter of the Electrical Engineering Department whose recommendations and interest kept me going through difficult times.

Most of the credit for this modest work must be given to my wife, Suzy. Her love and devotion, along with personal sacrifices, are what made this final product possible. It is to Suzy, and our three children, Suzanne, Kara, and John that this thesis is dedicated.

Contents

	Page
Preface	ii
List of Figures	v
List of Tables	vi
List of Notations	vii
Abstract	xi
I. Introduction	1
Background	1
Statement of the Problem	2
Assumptions	4
II. Formulation of Multipoint Boundary Value Problems	7
Coplanar Boundary Value Problems	8
Case One	12
Case Two	12
Case Three	13
Noncoplanar Boundary Value Problem	13
III. Numerical Algorithm	21
Background	21
Algorithm	21
ORBTRAN	22
NS01A	23
CALFUN	26
DFEQ	27
SLOPE	28
Program Integration	28
IV. Discussion of Results	31
Results of Coplanar Transfers	32

Contents

	Page
Thrust Termination	32
Effects of Varying Transfer Angle	37
Effect of Offloading Fuel	40
Effects of Changing Terminal Orbit Parameters	46
General Comments	47
Results of the Noncoplanar Transfers	51
Cross Check of Noncoplanar and Coplanar Transfers	51
Effect of Changing Inclination Angle	51
Use of Integration Scheme to Check Noncoplanar Problem	54
V. Conclusions	56
Bibliography	58
Appendix A: Coplanar Equations of Motion and Boundary Conditions	59
Appendix B: Noncoplanar Equations of Motion and Boundary Conditions	65
Appendix C: Derivation of Necessary Conditions	73
Appendix D: Computer Listing of Coplanar Problem	80
Appendix E: Computer Listing of Noncoplanar Problem	88
Vita	97

List of Figures

Figure		Page
1-1	The Space Shuttle Vehicle	1
3-1a	Numerical Algorithm Flow Chart	29
3-1b	Numerical Algorithm Flow Chart	30
4-1	Effect on Payload of Varying Transfer Angle ($e_f = 0$)	38
4-2	Effect on Payload of Varying Transfer Angle ($e_f \neq 0$)	39
4-3	Effect on Payload of Varying Transfer Angle ($p_f = 14,500$ nm)	41
4-4	Effect on Payload of Offloading (Geosynchronous Mission)	43
4-5	Effect on Payload of Offloading (12 Hour Mission) .	45
4-6	Time History of Control (Geosynchronous Mission)	48
4-7	Time History of Control (12 Hour Mission).	49
A-1	Coplanar Thrust Vector	60
B-1	Noncoplanar Transfer	65
B-2	Noncoplanar Thrust Vector	66
B-3	Spherical Coordinate System	67
B-4	Spherical Angles for Noncoplanar Problem.	70

List of Tables

Table		Page
I	Boeing Burner II Specifications	5
II	Summary of Coplanar MPBVPs	14
III	Summary of Noncoplanar MPBVPs	20
IVa	Results of Thrust Termination Problems	33
IVb	Results of Thrust Termination Problems	34
V	Varying p_f of Terminal Circular Orbit ($\theta = 180^o$).	46
VI	Maximum Payload Transfers to Elliptical Orbits	46
VII	Coplanar Solutions for Orbital Transfers (Case Three). .	50
VIII	Payload Check of Coplanar and Noncoplanar (i=0) Problems	53
IX	Effect of Inclination Angle on Payload ($\Delta t_1 = 120.89$). . . .	53
X	Results of Integration Scheme (i=10, $\theta' = 140$, $\Delta t_1 = 139.52$) .	55

List of Notation

English Symbols

ACC	convergence criterion
AFIT	Air Force Institute of Technology
C	effective exhaust velocity
CMU	canonical mass unit
CTU	canonical thrust unit
d( )	differential change
deg	degrees
DSTEP	step length used in search routine
DU	canonical distance unit
e	eccentricity
$\bar{e}$	unit vector
$\underline{f}$	error function vector
$\underline{F}$	force due to thrust
ft	feet
$\underline{G}$	force due to gravity
$\underline{h}$	specific angular momentum vector
H	hamiltonian
i	inclination angle between two orbits
I_{SP}	specific impulse

IUS	Interim Upper Stage
J	cost function
$\underline{J}$	Jacobian matrix
k	switching function
ℓ_i	direction cosine of thrust vector i=1, 2, 3
lbf	pounds-force
lbw	pounds-weight
m	vehicle mass
MPBVP	multipoint boundary value problem
nm	nautical mile
p	semi-latus rectum
r	radial distance from center of earth
r_A	radius at apogee
r_p	radius at perigee
$R_\oplus$	radius of earth
SAMSO	Space and Missile Systems Organization
sec	seconds
SRM	solid-rocket motor
SSV	Space Shuttle Vehicle
STS	Space Transportation System
t	time
t_1	time of first stage cutoff
t_2	time of second stage ignition
t_s	time of staging

T	thrust magnitude
TPBVP	two-point boundary value problem
TU	canonical time unit
u	control variable
USV	upper stage vehicle
V_R, V_θ, V_ϕ	velocity components in $\bar{e}_r, \bar{e}_\theta, \bar{e}_\phi$ directions respectively
$\underline{x}$	state variable vector
$\underline{y}$	vector of unknowns

Greek Symbols

α	thrust steering angle
β	spherical angle
γ	spherical angle
δ	a small variation
Δt_1	elapsed time for first stage burn
Δt_{1max}	maximum allowable time for first stage burn
Δt_2	elapsed time for second stage burn
Δt_{2max}	maximum allowable time for first stage burn
θ	central transfer angle in initial orbital plane measured counterclockwise from launch
θ'	central transfer angle in final orbital plane measured counterclockwise from launch
$\underline{\lambda}$	costate vector
μ	gravitational parameter
$\underline{\vartheta}$	lagrange multiplier vector associated with terminal conditions

$\underline{\pi}$	lagrange multiplier vector associated with constraints
ϕ	spherical angle measured clockwize from Z

Subscripts

actual	computed value
d	desired value
f	final value
o	initial value
$\underline{\ }$	vector quantity

Superscripts

$\underline{\ }$	unit vector
$\cdot$	first time derivative
$\cdot\cdot$	second time derivative
$\sim$	augmented function
*	optimal quantity

Abstract

A two-stage, solid-fuel proposal for the Interim Upper Stage Vehicle of the Space Transportation System has been selected for use by the Department of Defense. It is the purpose of this study to investigate the capabilities of such a vehicle in terms of the maximum payload which can be delivered to orbit. This optimal payload problem is examined in light of three energy management techniques. The first technique, thrust termination, involves shutting off engine thrust prior to complete use of propellant. The second technique investigates the effects on payload of varying the central angle through which the transfer is made. The third technique, offloading, examines the possibility of reducing the amount of available fuel for either stage prior to the mission to determine if payloads can be increased. Finite burn periods are assumed in this study. A multipoint boundary value problem results from the appearance of interior constraints in the problem. A numerical technique is used to generate solutions for a range of transfers in the special coplanar problem. Conclusions are discussed for each of the three energy management techniques in the coplanar transfer. Even though non-optimal noncoplanar results were obtained it is believed that the general coplanar results can be extended to the noncoplanar problem.

MAXIMUM PAYLOAD ORBITAL TRANSFERS FOR A SPACE SHUTTLE SOLID-FUEL UPPER STAGE VEHICLE

I. Introduction

Background

The Space Transportation System (STS) is a concept which is designed to reduce the costs of earth orbital operations and advance the capabilities of the United States in space. The STS consists of a Space Shuttle Vehicle (SSV), an upper stage vehicle (USV) and the necessary support systems. The SSV, depicted in Fig. 1-1, is designed to deliver scientific and defense satellites to earth orbits.

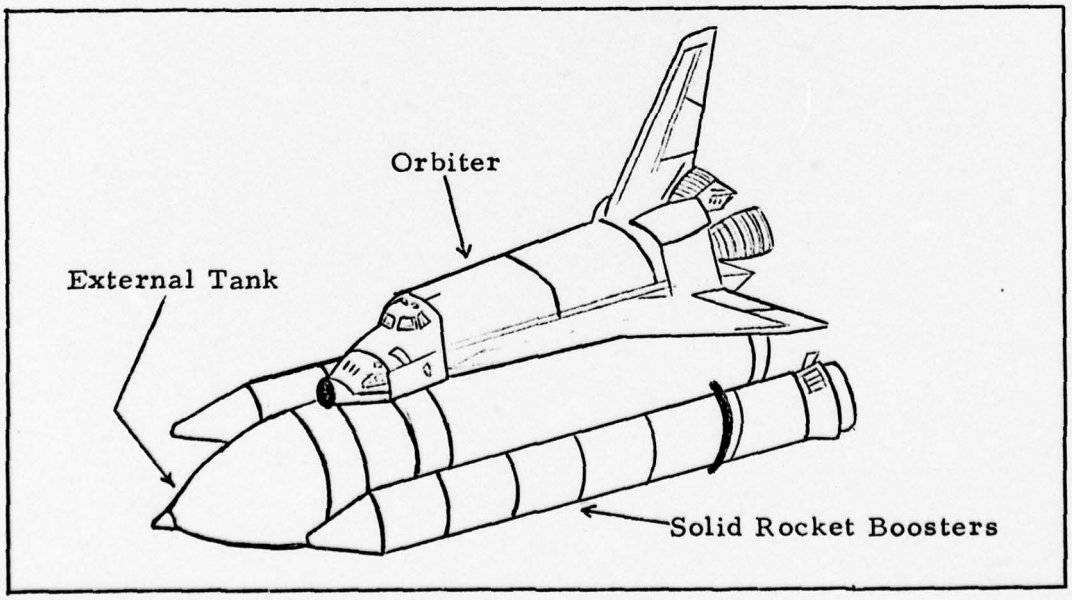

Fig. 1-1. The Space Shuttle Vehicle

The orbiter vehicle, shown in Fig. 1-1, is a reusable component of the SSV which is delivered to a low-Earth orbit through the use of an expendable external liquid-fuel tank and two reusable solid rocket boosters. The SSV has the capability to deliver the orbiter to low earth orbits of altitudes up to 500 nautical miles (nm). However, many of the missions for which the STS is designed require higher orbits. For these missions a propulsive upper stage vehicle (USV), which is carried in the cargo bay of the orbiter, is deployed by the orbiter in the low earth orbit. The USV is then used to deliver payloads beyond the capability of the orbiter vehicle. The STS was designed to relax the weight and volume constraints which previously have been placed on payloads transported to high earth orbits.

The USV that is presently being developed is the Interim Upper Stage (IUS). The IUS vehicle is capable of delivering single or multiple payloads to high earth orbits by use of a single IUS vehicle. Boeing's Burner II version of the IUS, a two-stage, solid-fuel vehicle, has been selected by the Space and Missile Systems Organization (SAMSO) for use in the initial phases of the Shuttle program.

Statement of the Problem

One way to examine the economical use of the IUS for an orbital transfer mission is to determine the maximum payload that can be delivered to orbit. This thesis addresses this maximum payload problem for one specific IUS vehicle. Three energy management techniques

are used to examine this optimization problem in an effort to study the capabilities of the IUS. The objective of this optimization problem is to determine the time history of the controls to give the maximum payload transfers.

The first technique, early thrust termination, implies incomplete use of the available propellant. This can be achieved by blowing off the engine nozzle or reducing the pressure in the combustion chamber of an engine. The two-stage IUS proposals submitted to SAMSO do not have this capability, but the concept is examined here to determine if discarding excess fuel in orbit would enable more payload to be delivered.

The second energy management scheme is offloading, that is, reducing the amount of propellant for a given stage prior to the mission. Examining the optimization problem with the added dimension of offloading provides a sizing analysis in terms of the maximum payload that can be delivered to orbit for different amounts of fuel. Thus for a specific payload, the "best" selection of available propellant loadings is possible.

The third energy management technique, varying the transfer angle, concedes the fact that there is excess fuel which must be carried and used. The question now becomes one of how to use that excess fuel. The present concept is to use a reaction control system to burn extra propellant. However, the concept of varying the transfer angle is presented here as an alternative to such an additional control system

which is designed to burn excess fuel.

The orbital transfers made in this study use finite periods of thrusting rather than the more common impulsive approximation of velocity changes. A finite burn is viewed as a more exact solution to the problem as it considers the fact that thrust direction may not be constant during thrusting periods. Another factor resulting in a more realistic solution for the finite burns is that the finite burn case considers the gravitational forces which must be overcome during periods of thrusting. The maximum payloads for the finite burn problem would thus be expected to be somewhat lower than those for the impulsive approximations.

Assumptions

Upon consideration of both solid- and liquid-fuel IUS proposals, SAMSO has granted a contract to Boeing Aerospace Company for its Burner II solid-rocket motor (SRM) version of the IUS. This particular two-stage vehicle does not have the capability to thrust terminate, so that concept, as developed in this study, pertains to future applications of such a vehicle. The vehicle, however, does presently have the capability of offloading fuel. The specifications of the Burner II vehicle can be found in Table I. It is assumed that the SRMs provide a constant thrust magnitude with a maximum amount of burning time for each stage.

Table I
Boeing Burner II Specifications

Stage 1 Summary	
Thrust	41,757.4 lbf
Specific Impulse	291.8 sec
Structure Weight	2,437.0 lbw
Propellant Weights	17,300.0 lbw
	or 19,967.0 lbw
Stage 2 Summary	
Thrust	14,076.6 lbf
Specific Impulse	300.8 sec
Structure Weight	1,362.0 lbw
Propellant Weight	4,700.0 lbw

The controls which we use to optimize the problem are the thrust directions. For the thrust termination problems, the numerical algorithm discussed in Chapter II also seeks the optimal times for first stage cutoff and second stage ignition. The equations which govern the motion of the vehicle are those as derived in an inverse-square gravitational field. Accelerations from sources other than the SRMs and the gravitational force of the earth are assumed to be negligible. The assumption is also made that changes in body attitude do not affect the motion of the vehicle.

For the orbital problems studied that involve transfers to final elliptical orbits, the major axis of the final orbit is assumed to be aligned with the point on the initial orbit at which the transfer begins. This assumption allows the true anomaly in the polar equation of a

conic orbit, Eq (A-16), to be equated to the central angle through which the transfer is made, θ.

The low earth parking orbit of the orbiter vehicle is assumed throughout this thesis to be a circular orbit around the earth at an altitude of 150 nm.

II. Formulation of Multipoint Boundary Value Problems

The objective of this study is to determine the time histories of the controls for a nonlinear system in such a manner that the initial mass is maximized subject to boundary constraints. The problem of thrust termination mentioned in Chapter I is atypical in that boundary constraints in this problem appear not only at initial and terminal points, but also at interior, or intermediate points. The initial constraints are given by the parameters of a parking orbit from which the mission begins. The terminal constraints are specified a priori and they define the orbit to which the transfer is made. The intermediate constraints pertain to physical parameters of the vehicle. Two of these interior constraints are placed on the maximum amount of time that each motor of the two-stage IUS can burn. A third interior constraint involves the mass which the vehicle jettisons at the staging point. These three inequality constraints are discussed in Appendix C. They necessitate the formulation of a multipoint boundary value problem (MPBVP) because of the possibility of discontinuities in the variables or equations at interior points.

It is also shown in Appendix C that three separate cases can be considered for the thrust termination problem. The first two cases are concerned with terminating thrust of one of the two IUS stages

before the propellant loaded for that stage has been completely used. The third case implies complete use of propellant in both stages. The problem of offloading fuel is covered by case three for which a different amount of propellant is assumed to be available for that stage.

The multi-point boundary value problem for each of the three cases that result from applying the necessary conditions of Appendix C are presented here.

Coplanar Boundary Value Problems

The state equations which govern the coplanar orbital transfer are derived in Appendix A and are as follows:

$$\dot{r} = V_R$$

$$\dot{\theta} = \frac{h}{r^2}$$

$$\dot{V}_R = \frac{h^2}{r^3} - \frac{\mu}{r^2} + \frac{T}{m} \sin \alpha \qquad (2\text{-}1)$$

$$\dot{h} = \frac{Tr}{m} \cos \alpha$$

$$\dot{m} = \frac{-T}{C}$$

where

r is the distance from the center of the earth

θ is the angle from the initial point to the present position

V_R is radial velocity

h is specific angular momentum

μ is the gravitational parameter

T is the magnitude of thrust

m is the vehicle's mass at a given time

α is the thrust steering angle measured clockwise from the local horizontal

C is the effective exhaust velocity

Since we want to maximize the payload for a fixed amount of propellant, the cost function, J, is:

$$J = -m(t_0) \tag{2-2}$$

where t_0 represents initial time. The mathematics of Appendix C seeks a minimum to this cost function. The minimum of a negative initial mass, with a fixed change in mass, is therefore the same as maximizing final mass. The Hamiltonian, H, is defined as:

$$H = \lambda_R V_R + \lambda_\theta \frac{h}{r^2} + \lambda_{V_R}\left[\frac{h^2}{r^3} - \frac{\mu}{r^2} + \frac{T}{m}\sin\alpha\right] + \lambda_h \frac{Tr}{m}\cos\alpha - \lambda_m \frac{T}{C} \tag{2-3}$$

where $\lambda_R, \lambda_\theta, \lambda_{V_R}, \lambda_h$, and λ_m are the costate variables.

Application of the optimality condition of Appendix C, Eq (C-21), and enforcement of the strengthened Legendre condition, yields the following expression for the thrust steering angles:

$$\sin \alpha = \frac{-\lambda_{V_R}}{P}$$

$$\cos \alpha = \frac{-\lambda_h r}{P} \qquad (2\text{-}4)$$

where $P = \sqrt{\lambda_{V_R}^2 + \lambda_h^2 r^2}$

The costate equations for this problem are defined by Eq (C-20). Substituting the controls of Eq (2-4) yields:

$$\dot{\lambda}_R = \frac{1}{r^3}\left[2\lambda_\theta h + \frac{3\lambda_{V_R} h^2}{r} - 2\lambda_{V_R}\mu\right] + \frac{\lambda_h^2 r T}{mP}$$

$$\dot{\lambda}_\theta = 0$$

$$\dot{\lambda}_{V_R} = -\lambda_R \qquad (2\text{-}5)$$

$$\dot{\lambda}_h = \frac{-1}{r^3}\left[\lambda_\theta r + 2\lambda_{V_R} h\right]$$

$$\dot{\lambda}_m = \frac{-TP}{m^2}$$

An initial circular parking orbit at an altitude above the earth of 150 nm is assumed throughout this study. The initial conditions are therefore:

$$r_0 = R_\oplus + 150 \text{ nm}$$

$$\theta_0 = 0 \qquad (2\text{-}6)$$

$$V_{R_0} = 0$$

$$h_0 = \sqrt{\mu r_0} \tag{2-6}$$

where $R_\oplus$ is the radius of the earth and $(\ )_o$ denotes value at the initial point. Another initial condition is given for the mass costate by Eq (C-17) as:

$$\lambda_{m_0} = 1 \tag{2-7}$$

The terminal constraints are repeated here from the derivation in Appendix C:

$$r_f = \frac{p_f}{1 + e_f \cos \theta_f}$$

$$\theta_f \text{ - specified}$$

$$V_{r_f} = \frac{e_f h_f \sin \theta_f}{p_f} \tag{2-8}$$

$$h_f = \sqrt{\mu p_f}$$

where $(\ )_f$ denotes the value at the final time, p is the semi-latus rectum and e is eccentricity. We also know from the transversality conditions derived in Appendix C that the mass costate at the final time is given by:

$$\lambda_m(t_f) = 0 \tag{2-9}$$

The remainder of the boundary value problem must be developed for each of the three cases described in Appendix C.

Case One. This case is characterized by incomplete use of the second stage fuel while the first stage is completely burned. The necessary conditions unique to this problem are described by Eq (C-11). From these conditions we know the value of the Hamiltonian at the final time is:

$$H(t_f) = 0 \tag{2-10}$$

It is also known that the Hamiltonian is continuous at second stage ignition. The partial derivative of the Hamiltonian with respect to thrust at that time must therefore be zero. The expression described by this relationship is known as the switching function. The equation is:

$$\frac{\partial H}{\partial T} = k = -\left[\frac{P}{m} + \frac{\lambda m}{C}\right] = 0 \text{ at } t_2 \tag{2-11}$$

where t_2 is the time of second stage ignition.

This MPBVP is summarized in Table II. It can be seen that a solution to this problem with twelve equations and twelve unknowns is possible.

Case Two. This case involves thrust termination of only the first stage of the IUS. The necessary conditions derived in Appendix C, Eq (C-13) yields the following condition:

$$H(t_f) = H_4(t_2) - H_3(t_2) \qquad (2\text{-}12)$$

where $H_3(t_2)$ is the Hamiltonian just prior to second stage ignition and $H_4(t_2)$ is the Hamiltonian an instant after ignition of the second stage. The Hamiltonian being continuous at the first stage cutoff, t_1, yields:

$$\frac{\partial H}{\partial T} = k = -\left[\frac{P}{m} + \frac{\lambda m}{C}\right] = 0 \text{ at } t_1 \qquad (2\text{-}13)$$

The boundary value problem is summarized in Table II.

Case Three. The third case, which serves as a basis of comparison for the other two cases, involves the complete burning of all loaded propellant in the IUS. The comparison with the case three problem is used to indicate if thrust termination of either stage yields any extra payload. This case is also used for the analysis of offloading fuel. The associated necessary condition derived in Appendix C is:

$$H(t_f) = H_4(t_2) - H_3(t_2) \qquad (2\text{-}14)$$

Since the Hamiltonian is discontinuous at both t_1 and t_2, there is no equation involving the switching function. The MPBVP is given in Table II. As in the other two cases, it can be seen that the number of unknowns match the number of equations.

Noncoplanar Boundary Value Problem

The general problem of a noncoplanar orbital transfer is depicted in Fig. B-1. The appropriate state equations for this problem as derived in Appendix B are:

Table II
Summary of Coplanar MPBVPs

Elements of MPBVP	Case 1		Case 2		Case 3	
	Unknowns	Equations	Unknowns	Equations	Unknowns	Equations
State Equations Eq. (2-1)	5 Constants of Integration		5 Constants of Integration		5 Constants of Integration	
Costate Equations Eq. (2-5)	5 Constants of Integration		5 Constants of Integration		5 Constants of Integration	
Initial Conditions Eq. (2-6), (2-7)		r_o, θ_o, V_{R_o} h_o, $\lambda_{m_o} \rightarrow$ Eq (2-7)		r_o, θ_o, V_{R_o} h_o, $\lambda_{m_o} \rightarrow$ Eq (2-7)		r_o, θ_o V_{R_o}, h_o $\lambda_{m_o} \rightarrow$ Eq (2-7)
Intermediate Conditions Eq. (C-2), (C-3), (C-4)	t_2	$k(t_2)=0$ Eq (2-11)	t_1	$k(t_1)=0$ Eq (2-13)		
Terminal Conditions Eq (2-8)	t_f	r_f, θ_f, V_{r_f} $h_f, \lambda_m(t_f)$ $\rightarrow$ Eq (2-9) $H(t_f) \rightarrow$ Eq (2-10)	t_f	r_f, θ_f, V_{R_f} $h_f, \lambda_m(t_f)$ $\rightarrow$ Eq(2-9) $H(t_f) \rightarrow$ Eq (2-12)	t_f	r_f, θ_f, V_{R_f} $h_f, \lambda_m(t_f)$ $\rightarrow$ Eq (2-9) $H(t_f) \rightarrow$ Eq (2-14)
Total	12	12	12	12	11	11

$$\dot{r} = V_R$$

$$\dot{\theta} = \frac{V_\theta}{r}$$

$$\dot{\phi} = \frac{V_\phi}{r} \qquad (2\text{-}15)$$

$$\dot{V}_R = \frac{V_\phi^2}{r} + \frac{V_\theta^2}{r} \sin^2\phi - \frac{\mu}{r^2} + \frac{T\ell_1}{m}$$

$$\dot{V}_\theta = \frac{-V_R V_\theta}{r} \frac{-2V_\theta V_\phi}{r} \cot\phi + \frac{T\ell_2}{m \sin\phi}$$

$$\dot{V}_\phi = \frac{-V_R V_\phi}{r} \frac{+V_\theta^2 \sin\phi}{r} \cos\phi + \frac{T\ell_3}{m}$$

$$\dot{m} = -\frac{T}{C}$$

where r is the radius from the earth's center to the IUS

θ is the transfer angle measured in the initial orbital plane

ϕ is the angle measured from the vertical axis to the vehicle.

V_R, V_θ, and V_ϕ are the velocity state variables

m is the vehicle's mass at a given time

μ is the gravitational parameter

T is thrust magnitude

ℓ_1, ℓ_2, and ℓ_3 are the direction cosines of the thrust vector

With the cost function, J, for this problem defined as

$$J = -m(t_o) \qquad (2\text{-}16)$$

the Hamiltonian becomes:

$$H = \lambda_R V_R + \lambda_\theta \frac{V_\theta}{r} + \frac{\lambda_\phi V_\phi}{r} + \lambda_{V_R} \left[\frac{V_\phi^2}{r} + \frac{V_\theta^2 \sin^2\phi}{r} - \frac{\mu}{r^2} + \frac{T\ell_1}{m} \right]$$

$$+ \lambda_{V_\theta} \left[\frac{-V_R V_\theta}{r} \frac{-2V_\theta V_\phi}{r} \cot\phi + \frac{T\ell_2}{m \sin\phi} \right] \qquad (2\text{-}17)$$

$$+ \lambda_{V_\phi} \left[\frac{-V_R V_\phi}{r} + \frac{V_\theta^2 \sin\phi\cos\phi}{r} + \frac{T\ell_3}{m} \right] - \lambda_m \frac{T}{C}$$

where $\lambda_R, \lambda_\theta, \lambda_\phi, \lambda_{V_R}, \lambda_{V_\theta}, \lambda_{V_\phi}$ and λ_m are the costates associated with the state variables.

As in the coplanar problem, the optimality necessary condition and the strengthened Legendre-Clebsch condition applied to the Hamiltonian yield the following expressions for the thrust directions:

$$\ell_1 = \frac{-\lambda_{V_R}}{P}$$

$$\ell_2 = \frac{-\lambda_{V_\theta}}{P \sin\phi} \qquad (2\text{-}18)$$

$$\ell_3 = \frac{-\lambda_{V_\phi}}{P}$$

where $P = \sqrt{\lambda_{V_R}^2 + \left(\frac{\lambda_{V_\theta}}{\sin\phi} \right)^2 + \lambda_{V_\phi}^2}$ (2-19)

The necessary condition for the costates, defined by Eq (C-20), is applied to the above Hamiltonian with the expressions for thrust direction substituted in the proper places. The results are:

$$\dot{\lambda}_R = \frac{1}{r^2}\left[\lambda_\theta V_\theta + \lambda_\phi V_\phi + \lambda_{V_R}\left(V_\phi^2 + V_\theta^2 \sin^2\phi - 2\frac{\mu}{r}\right)\right.$$

$$\left. - \lambda_{V_\theta}\left(V_R V_\theta + 2 V_\theta V_\phi \cot\phi\right) - \lambda_{V_\phi}\left(V_R V_\phi - V_\theta^2 \sin\phi\cos\phi\right)\right]$$

$$\dot{\lambda}_\theta = 0$$

$$\dot{\lambda}_\phi = \frac{-2\lambda_{V_R} V_\theta^2}{r} \sin\phi\cos\phi - \frac{2\lambda_{V_\theta} V_\theta V_\phi}{r \sin^2\phi} - \frac{\lambda_{V_\theta}^2 T \cos\phi}{m P \sin^3\phi} - \frac{\lambda_{V_\phi} V_\theta^2}{r}\left(\cos^2\phi - \sin^2\phi\right)$$

$$\dot{\lambda}_{V_R} = \frac{1}{r}\left[\lambda_{V_\theta} V_\theta + \lambda_{V_\phi} V_\phi\right] - \lambda_R \qquad (2\text{-}20)$$

$$\dot{\lambda}_{V_\theta} = -\frac{1}{r}\left[\lambda_\theta + 2\lambda_{V_R} V_\theta \sin^2\phi - \lambda_{V_\theta} V_R - 2\lambda_{V_\theta} V_\phi \cot\phi + 2\lambda_{V_\phi} V_\theta \sin\phi\cos\phi\right]$$

$$\dot{\lambda}_{V_\phi} = \frac{1}{r}\left[\lambda_\phi - 2\lambda_{V_R} V_\phi + 2\lambda_{V_\theta} V_\theta \cot\phi + \lambda_{V_\phi} V_R\right]$$

$$\dot{\lambda}_m = -\frac{TP}{m^2}$$

The assumption of an initial circular parking orbit once again defines some of the initial conditions as shown below. The terminal conditions derived in Appendix C are also shown here.

$$r_o = R_\oplus + 150 \text{ nm}$$

$$\theta_o = 0$$

$$\phi_o = 90^\circ$$

$$V_{R_o} = 0 \qquad (2\text{-}21)$$

$$V_{\theta_o} = \sqrt{\frac{\mu}{r_o}}$$

$$V_{\phi_o} = 0$$

$$r_f = \frac{pf}{1 + e_f \cos \theta'_f}$$

$$\phi_f = \phi_o + \sin^{-1} (\cos \theta'_f \sin i)$$

$$\theta_f = \cos^{-1} \left[\frac{\tan \phi_f}{\tan i}\right] \qquad (2\text{-}22)$$

$$V_{R_f} = \frac{e_f h_f \sin \theta'_f}{p_f}$$

$$V_{\theta_f} = \frac{h_f}{r_f} (\cos i - \sin i \cos \theta_f \cot \phi_f)$$

$$V_{\phi_f} = \frac{-h_f}{r_f} \sin i \sin \theta_f$$

where $(\ )_o$ indicates value at initial point

$(\ )_f$ denotes value at terminal point

θ'_f is the transfer angle in the plane of the terminal orbit

h is angular momentum

e is eccentricity

i is the inclination angle between the initial and final orbits

Additional boundary conditions on the mass costate are derived in Appendix C. Those boundary conditions are:

$$\lambda_m (t_o) = 1 \tag{2-23}$$

$$\lambda_m(t_f) = 0 \tag{2-24}$$

As in the coplanar problem, a specific set of necessary equations exists for each of the three classes of problems studied here. The reader is referred to the formulation of the coplanar MPBVP earlier in the chapter for an explanation of those additional necessary conditions. A summarization of the MPBVP for the nonplanar case is found in Table III.

Table III
Summary of Noncoplanar MPBVPs

Elements of MPBVP	Case One		Case Two		Case Three	
	Unknowns	Equations	Unknowns	Equations	Unknowns	Equations
State Equations Eq (2-15)	7 Constants of Integration		7 Constants of Integration		7 Constants of Integration	
Costate Equations Eq (2-20)	7 Constants of Integration		7 Constants of Integration		7 Constants of Integration	
Initial Conditions Eq (2-21)		r_o, θ_o, ϕ_o, V_{R_o}, V_{θ_o}, V_{ϕ_o} $\lambda_m(t_o) \rightarrow$ Eq (2-23)		r_o, θ_o, ϕ_o, V_{R_o}, V_{θ_o}, V_{ϕ_o} $\lambda_m(t_o) \rightarrow$ Eq (2-23)		r_o, θ_o, ϕ_o, V_{R_o}, V_{θ_o}, V_{ϕ_o} $\lambda_m(t_o) \rightarrow$ Eq (2-23)
Intermediate Conditions Eq (C-2), (C-3), (C-4)	t_2	$k(t_2) = 0$ Eq (2-1)	t_1	$k(t_1) = 0$ Eq (2-13)		
Terminal Conditions Eq (2-22)	t_f	r_f, θ_f, ϕ_f V_{r_f}, V_{θ_f}, V_{ϕ_f} $\lambda_m(t_f) \rightarrow$ Eq (2-24) $H(t_f) \rightarrow$ Eq (2-10)	t_f	r_f, θ_f, ϕ_f V_{r_f}, V_{θ_f}, V_{ϕ_f} $\lambda_m(t_f) \rightarrow$ Eq (2-24) $H(t_f) \rightarrow$ Eq(2-12)	t_f	r_f, θ_f, ϕ_f V_{r_f}, V_{θ_f}, V_{ϕ_f} $\lambda_m(t_f) \rightarrow$ Eq (2-24) $H(t_f) \rightarrow$ Eq (2-14)
Total	16	16	16	16	15	15

III. Numerical Algorithm

Background

Having derived the necessary conditions for an optimal trajectory and formulated a MPBVP, a method to find a solution for the problem must now be generated. The necessary conditions given in Chapter II must be satisfied at each point in the time interval of interest. A closed-form solution of this problem could not be found. Therefore, a numerical technique is used to search for the unknowns such that the necessary equations and boundary conditions are satisfied. That which follows is an explanation of the numerical algorithm developed to solve the MPBVP.

Algorithm

Due to the possibility of discontinuities in the problem variables, the MPBVP formulated in Chapter II is separated into three related parts that can be implemented in a computer. The first part covers the first thrusting period from the initial point to first stage cutoff at time t_1. The next portion covers the coasting period of the trajectory from first stage cutoff until second stage ignition. It is during this time interval that staging occurs. The last of the three parts includes the second stage burning period. The endpoint of this problem signifies the final time, t_f, at which point the terminal

boundary conditions must be satisfied.

The numerical algorithm formulated in this thesis consists of several routines which perform unique functions within the main algorithm. An explanation of the processing involved in those routines and the program integration are included in this chapter.

ORBTRAN. This routine in the main program sets up a normalization routine, accepts input data, and forms an initial guess for the unknowns. ORBTRAN also initiates the calls to the subroutines in the program.

The normalization routine used in this study is similar to the scheme proposed in Ref 3. All distance, velocity, time, mass and thrust units in this problem are divided by canonical units prior to their use in the search routine. The distance unit, DU, represents the radius of the earth. A circular reference orbit is assumed just above the surface of the earth. Velocity and time canonical units are therefore defined by the speed of a hypothetical satellite in that reference orbit. The gravitational parameter, μ, is therefore $1 \frac{DU^3}{TU^2}$. Consistent mass and thrust units are also developed. The mass unit, CMU, that provided the best convergence was 5000 lb-sec^2/ft. The thrust unit, CTU, was defined as follows

$$1 \text{ CTU} = 1 \text{ CMU} \times \frac{1DU}{1TU^2} \tag{3-1}$$

The next main function of ORBTRAN is to receive inputs in the form of vehicle parameters, initial conditions, and terminal

conditions. Specific impulses of each stage are input to ORBTRAN. These values are used to determine the effective exhaust velocities for the motors.

The initial conditions for the problem are determined from the parking orbit parameters which are input to ORBTRAN. Those parameters are eccentricity and semi-latus rectum. Terminal conditions are determined in ORBTRAN by inputs of the transfer angle, semi-latus rectum and eccentricity of the desired terminal orbit. The equations for the terminal conditions listed in the Appendices are used to determine the values the states should have at t_f. All boundary conditions are then normalized within ORBTRAN.

Initial guesses of the unknowns are input to the main program. Once the correct values of the unknowns have been determined for a particular mission those values are then used as inputs for another similar orbital transfer. This recursive use of the algorithm provides good guesses for the unknowns and thus significantly reduces the required computational time. ORBTRAN receives as outputs from NS01A the values of the unknowns that yield a solution to the MPBVP.

NS01A. This subroutine, which is on permanent file at the AFIT computer, was developed by M. J. D. Powell. (See Ref 7). NS01A receives as inputs a vector of unknowns, $\underline{x}$, and several parameters which direct its operation. The algorithm was developed

to numerically solve a system of n non-linear equations in n unknowns:

$$\underline{f}_k(x_1, x_2, x_3 \ldots x_n) = 0 \quad k = 1, \ldots, n \tag{3-2}$$

where $\underline{f}$ is a vector of error functions (non-linear equations) in the unknown parameters, x_i. It is claimed in Ref 7 that this algorithm maintains a fast convergence rate in addition to the capability to achieve convergence if initial guesses of the unknowns are poor estimates.

NS01A calculates the Jacobian matrix, $\underline{J}$, of the error function:

$$\underline{J} = \frac{\partial}{\partial \underline{x}} \underline{f}(\underline{x}) \tag{3-3}$$

A Newton-Raphson step gives:

$$f(\underline{x}) + \underline{J}\,\delta\,\underline{x} = 0 \tag{3-4}$$

where $\delta\underline{x}$ is a correction to $\underline{x}$. It is therefore possible to find a $\delta\underline{x}$ for a given step length so that the following equation is met:

$$f(\underline{x} + \delta\underline{x}) < \underline{f}(\underline{x}) \tag{3-5}$$

A correction vector is found at each iteration until the desired accuracy is achieved, that is:

$$\sum_{K=1}^{n} [\underline{f}_K(\underline{x})]^2 < ACC$$

For this thesis, with the variables normalized to canonical units, ACC was specified as 10^{-12}.

Another important parameter in NS01A which must be properly chosen to insure convergence is the increment size for the unknowns, DSTEP. A step length that is too small would require an excessive number of iterations to achieve convergence. On the other hand, DSTEP must be small enough to insure that Eq (3-5) is satisfied at each iteration. A value of 10^{-7} for DSTEP proved to be the best choice for the problems of this thesis.

The unknowns in the problem, $\underline{x}$, are all incremented at the same constant DSTEP within NS01A. The proper scaling of those unknowns is therefore required. Improper scaling could result in a negligible change in the error functions at each increment in the unknowns, (see Eq (3-3)). Such a result would make convergence to the proper solution nearly impossible. For example, it was determined early in the study that the MPBVP was very sensitive to changes in the initial costates. They had to be incremented with a DSTEP of 10^{-7}. Such a change in the unknown initial mass parameter at each iteration would yield negligible changes in the error functions due to that parameter since it has a value in the range of 30,000 lbw. Convergence to a solution would be virtually impossible in this case. The normalization scheme mentioned earlier places the proper significance on the increment size for the unknowns at each iteration and thus eliminates some of the convergence difficulties.

NS01A internally calls subroutine CALFUN which is used to find the error functions. A more detailed description of NS01A can be found in Ref 7.

CALFUN. The main task of this subroutine is to provide an error function, f, for use in NS01A. The components of the error function are determined from the difference between the desired and computed values of the equations for a specific case of the MPBVP. For example for case three of the coplanar problem we have

$$f_2 = \theta_{f_d} - \theta_{f_{actual}}$$

where θ_{f_d} and $\theta_{f_{actual}}$ are the desired and computed values for the transfer angle.

As inputs CALFUN receives the desired values of the boundary conditions, the initial guesses on the unknowns and the vehicle parameters. CALFUN then acts in an executive manner to integrate the differential state and costate equations for each portion of the trajectory. The actual values of the states which are required for the error functions are then extracted from the integration routine at the proper points.

The integration routine in CALFUN includes three different calls to the integration scheme. The first call is related to the first thrusting period. First stage thrust magnitude, effective exhaust velocity and t_1 are required for this routine. The switching function, $k(t_1)$ is determined at the end of the first portion of the MPBVP.

The next portion of the MPBVP, representing the coast period, receives the final values of the states and costates from the first part as starting values. Thrust and effective exhaust velocity are both zero during coasting. Upon initialization of these differential equations, the first stage structure weight is subtracted from the mass state variable. At the end of this period at t_2, the switching function, $k(t_2)$, and Hamiltonian, $H_3(t_2)$ are determined.

The final values from the coasting period are used as inputs for the states and costates in the third portion of the MPBVP. The Hamiltonian, $H_4(t_2)$, is determined after this portion of the MPBVP is initialized. Since this phase covers second stage thrusting, the appropriate thrust and effective exhaust velocity must be provided. The required terminal boundary conditions, $\lambda_m(t_f)$, and $H(t_f)$ are determined at the endpoint of this problem.

DFEQ. This routine is also on permanent file at the AFIT computer. It is comprised of two subroutines, SET and STEP. These subroutines accomplish the integration of the first-order differential equations in the problem. The inputs required by these subroutines are the initial values, total integration time, and step size. SET is first called to initialize the integration scheme. Then STEP is called to integrate the equations of motion through a time interval, DT. A Runge-Kutta method is used to integrate over three steps after the initial point is determined by SET. A fourth-order Adams-Bashforth-Adams-Moulton predictor-corrector scheme is

then applied to the next two points. This procedure uses the equations from subroutine SLOPE to integrate over the entire interval, t.

SLOPE. Subroutine slope sets up the differential state and costate equations as derived in Chapter II. The equations are general in nature so they may be used for either thrust or coast periods of a trajectory. The inputs to this subroutine are the values of the states and costates at a given time when called from DFEQ. This subroutine computes the slope of a given state or costate which is subsequently used by DFEQ to estimate the value of that parameter at some future time, $t + \Delta t$.

Program Integration

The overall integration of these subroutines to comprise the numerical algorithm can be seen in Fig. 3-1. The main program, ORBTRAN, performs the executive function of the algorithm. It provides the call to the search routine, NS01A. That routine then changes the initial guesses of the unknowns such that the error function decreases in magnitude. Internal to NS01A is a call to CALFUN which directs the integration routine so that the error function can be determined. NS01A repeatedly calls CALFUN until the error function is within the desired accuracy. The outputs of NS01A are the unknowns which yield the desired accuracy in the error function.

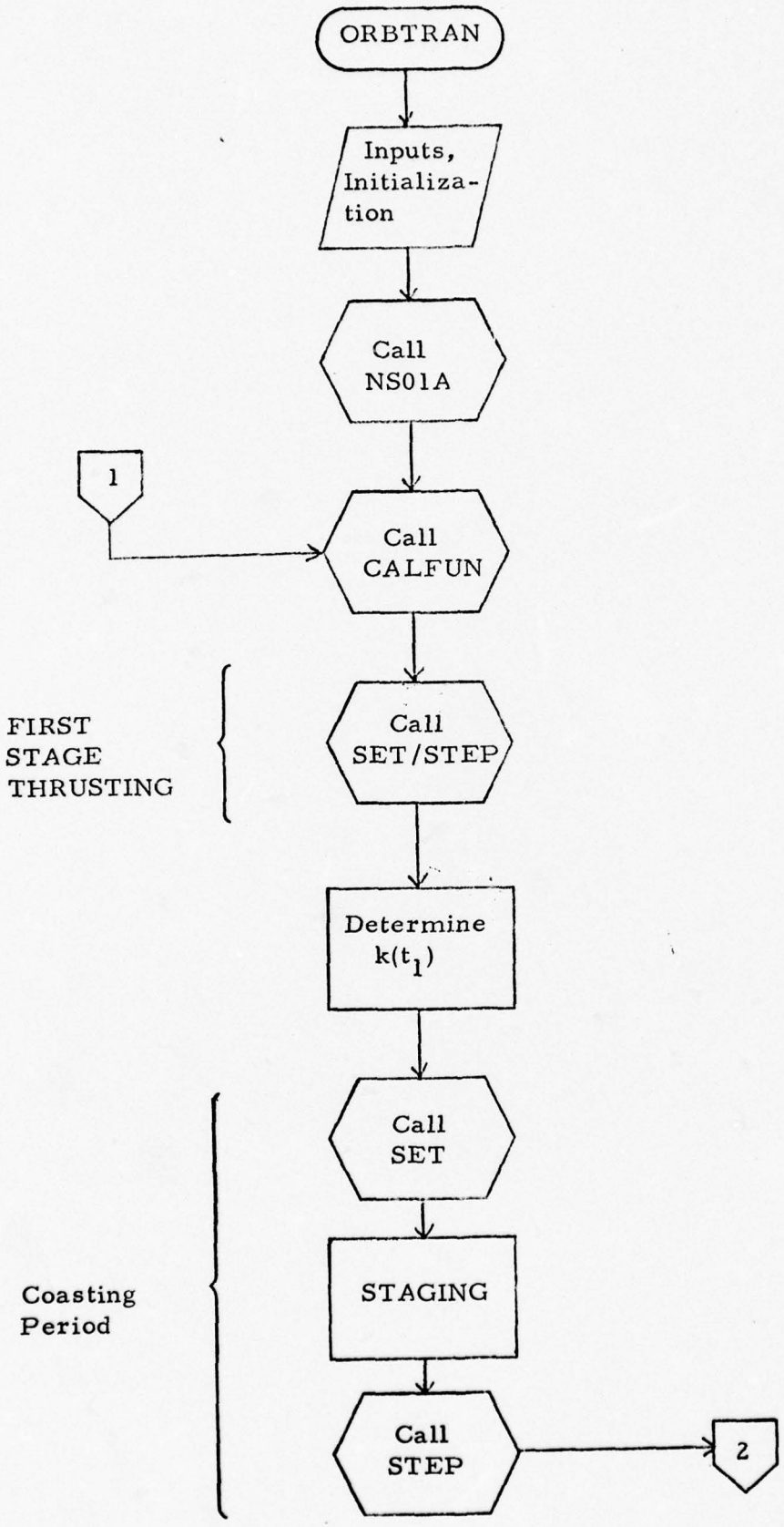

Fig. 3-1a. Numerical Algorithm Flow Chart

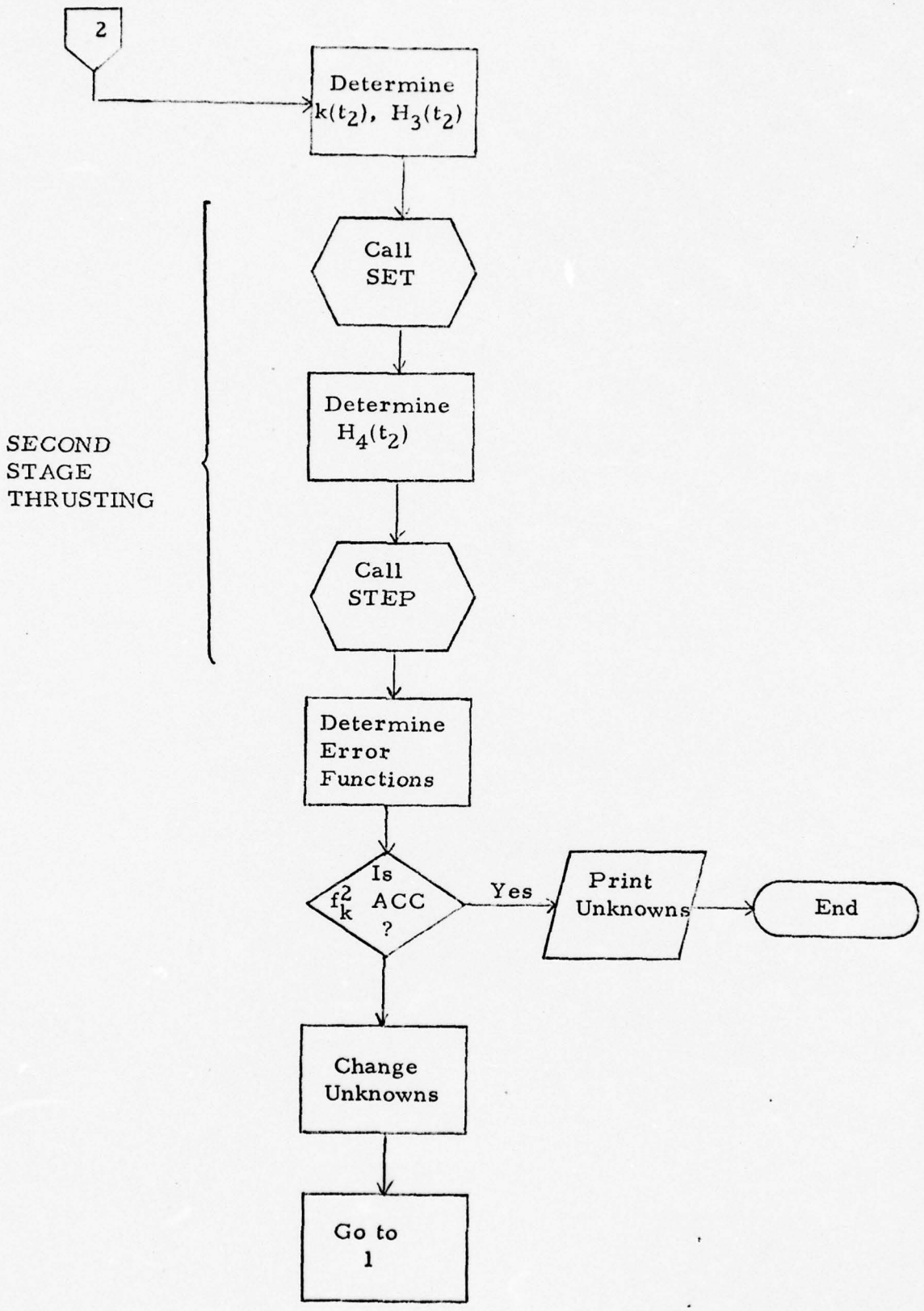

Fig. 3-1b. Numerical Algorithm Flow Chart

IV. Discussion of Results

Convergence to a solution to the MPBVP proved to be very sensitive to changes in the initial estimates of the unknowns. Those unknowns include the initial values of the costates and the unknown times. The algorithm failed to converge to a solution for poor guesses of those unknowns. The differences between the desired and computed values of the terminal conditions were not within acceptable limits when poor initial estimates of the unknowns were used. Since physical reasoning could not be used to obtain guesses for the λ unknowns, a great deal of computer time was required to achieve convergence for the initial problem. Once a solution was obtained, however, the correct values of the unknowns were used as inputs for a similar mission with a small change in the transfer angle or in the radius. In this manner a range of solutions were obtained.

Both the coplanar and noncoplanar results are presented in this chapter. Analytical justifications and validation of results are also included. The maximum payload orbital transfer results are presented for the two primary design reference missions of the IUS. The first of these is a transfer to a circular geosynchronous orbit at an altitude of 19,323 nm. The second mission, known as the 12 hour mission, defines the terminal orbit as an elliptical orbit with

an apogee altitude of 21,450 nm and a perigee altitude of 350 nm. The results are also presented for the two main first stage propellant loadings listed in Table I. The first loading of 19,967 pounds gives a maximum burn time of 139.52 seconds, while the 17,300 pound loading enables 120.89 seconds of first stage burn.

Results of Coplanar Transfers

Results for each of the three energy management techniques were obtained for the coplanar transfer problem.

Thrust Termination. At the beginning of this study, it was believed that the ability to thrust terminate might be desirable in terms of increasing payload capability. However, successful orbital transfers were not obtained for either the case one or case two problem. Numerous approaches were attempted to obtain a solution to the thrust termination cases. The missions were changed to determine if thrust termination could produce solutions for only a certain class of missions. Different sets of the initial estimates of the unknown costates were used as inputs, but to no avail. The best accuracies that could be achieved for either case of thrust termination were obtained by using the values of the unknowns for a successful case three transfer in which all the fuel was used. Those results appear in Table IV. It is apparent from an examination of the burning times and initial masses listed in the table for the case one and case two problems that, even when case three results are input to the

Table IVa
Results of Thrust Termination Problems

Mission	Unknowns	Case 1 * $\Delta t_1 = \Delta t_{1max}$ $\Delta t_2 < \Delta t_{2max}$	Case 2 * $\Delta t_1 < \Delta t_{1max}$ $\Delta t_2 = \Delta t_{2max}$	Case 3 * $\Delta t_1 = \Delta t_{1max}$ $\Delta t_2 = \Delta t_{2max}$
Geosynchronous	λ_R	.09098	.10675	.09097
	λ_θ	.00572	.00685	.00571
	λ_{V_R}	-.00621	-.00609	-.00619
$e_f = 0$	λ_h	-.37017	-.43392	-.37012
p_f = 19,323 nm.	$m(t_0)$ (lbs)	30,189.	35,609.	30,189.
$\theta = 180^o$	t_1** (sec)	120.89	142.95	120.89
	t_2** (sec)	17,428.79	17,234.35	17,435.24
	t_f** (sec)	17,532.06	17,334.75	17,535.64
	accuracy	.8577E-4	.2288E2	.1E-12
12 Hour Mission	λ_R	.08273	.08270	.08270
	λ_θ	.00529	.00531	.00531
	λ_{V_R}	-.00532	-.00538	-.00538
e_f = .593	λ_h	-.32927	-.32919	-.32920
p_f = 8088 nm.	$m(t_o)$ (lbs)	29,156.	29,157.	29,158.
$\theta = 180^o$	t_1** (sec)	120.89	120.88	120.89
	t_2** (sec)	23,079.71	23,117.63	23,016.78
	t_f** (sec)	23,132.15	23,218.04	23,117.18
	accuracy	.3649E-5	.215E2	.1E-12

* Δt_1 = elapsed time for first stage burn
Δt_{1max} = maximum time for first stage burn
Δt_2 = elapsed time for second stage burn
Δt_{2max} = maximum time for second stage burn

** t_1 = time of first stage shutoff
t_2 = time of second stage ignition
t_f = time of orbit insertion

Table IVb
Results of Thrust Termination Problems

Mission	Unknown	Case 1 * $\Delta t_1 = t_{1max}$ $\Delta t_2 < t_{2max}$	Case 2 * $\Delta t_1 < t_{1max}$ $\Delta t_2 = t_{2max}$	Case 3* $\Delta t_1 = t_{1max}$ $\Delta t_2 = t_{2max}$
Geosynchronous $e_f = 0$ $p_f = 19,323$ nm. $\theta = 140^\circ$	λ_r	.04165	.00821	.04124
	λ_θ	.04435	.09095	.04431
	λ_{V_R}	-.09262	-.19137	-.09259
	λ_h	-.24638	-.27455	-.24500
	$m(t_o)$ (lbs)	27,142.	37,642.	27,140.
	t_1** (sec)	120.89	172.37	120.89
	t_2** (sec)	9,900.41	11,487.41	9,908.48
	t_f** (sec)	10,004.49	11,587.81	10,008.88
	accuracy	.9859E-3	.1538E2	.1E-12
12 Hour Mission $e_f = .593$ $p_f = 8,088$ nm. $\theta = 140^\circ$	λ_r	.04407	.01043	.04403
	λ_θ	.04570	.27058	.04554
	λ_{V_R}	-.09688	-.98760	-.09656
	λ_h	-.26202	-2.0377	-.26156
	$m(t_o)$ (lbs)	27,518.	329,510.	27,528.
	t_1** (sec)	120.89	2,062.94	120.89
	t_2** (sec)	9,186.38	6,428.69	9,140.39
	t_f** (sec)	9,238.82	6,529.09	9,240.79
	accuracy	.2041E-4	.3606E1	.1E-12

*Δt_1 = elapsed time for first stage burn
Δt_{1max} = maximum time for first stage burn
Δt_2 = elapsed time for second stage burn
Δt_{2max} = maximum time for second stage burn

** t_1 = time of first stage shutoff
t_2 = time of second stage ignition
t_f = time of orbit insertion

thrust termination problems, the algorithm does not always drive towards the case three solution. For instance, the case one problem for a 12 hour mission with $\theta = 180^{o}$ shows a second stage burn of about 52 seconds which is far below that burning constraint. The established convergence criterion was never achieved for the thrust termination problems. If early thrust termination is not optimal, it appears that a solution should at least have been obtained by the algorithm driving to the limiting case three solution. The reason for the failure of the algorithm to provide such solutions most probably lies in the fact that case one and case two have error functions which include switching functions. The sensitivity of these functions to the costate values at a particular time is very great, as discovered in Ref 6. The error function in the algorithm involving the switching function was the primary contribution to the relatively high value of final accuracy which was on the order of 10^{-5} for the case one problem. For the problems involving those additional necessary conditions it was therefore not possible to achieve the desired accuracy.

A variety of missions and transfer angles were tested with the results being similar to those in Table IV. Both of the first stage propellant loadings were also tested. Convergence to a solution failed in every instance.

Although convergence to a solution was not obtained for the thrust termination problems, an analytical argument is presented here to support the fact that thrust termination cannot increase

payload capability. Solutions to the case three problem are available for fuel loadings which are less than the maximum loadings. Those results can be used to determine if case one or case two can increase payload. For example, with 18,900 lbs of first stage fuel and 4,700 lbs of second stage fuel (maximum second stage loading), the case three payload capability is about 5,100 lbs. If the second stage loading is decreased to 4,400 lbs for the same first stage loading, the case three problem indicates that the final mass is increased to 5,300 lbs. In the case one analysis of this latter problem, however, the burning of 4,400 lbs of fuel is interpreted as incomplete use of available second stage propellant. This means that 300 lbs of the final mass is unused fuel, or deadweight. The payload is therefore 5,000 lbs. This indicates a decrease in payload when all available fuel is not used. This result, which consistently holds in such an analysis for decreasing second stage burn, shows that terminating second stage thrusting early will not increase payload capability. The optimal solution to the case one problem, which has the possibility to use less than all the loaded second stage fuel, is always to use the maximum amount of available fuel.

Similar results are obtained in the analysis of the case two problem. Terminating the first burn early decreases the payload capability. For example, with the maximum first and second stage fuel being used approximately 5,900 lbs of payload can be delivered. Keeping the second stage burn time constant and terminating first

stage thrusting 7.52 seconds early decreases the final mass to 5,100 lbs. Subtracting the unused first stage fuel from the final mass yields a payload of 4,000 lbs. The conclusion that can be arrived at is that the optimal solution to the case two problem is to burn the maximum amount of time on the first burn.

Effects of Varying Transfer Angle. In contrast to the thrust termination problems, a variety of solutions were obtained for the third case of the multi-point boundary value problem. Thus the other two energy management techniques of varying transfer angle and off-loading fuel can be examined. One cross-check of the accuracy of this problem was obtained by a comparison with the Hohmann transfer problem. For both first stage propellant loadings the Hohmann approximation for the initial mass was within one percent of the maximum initial mass for the finite burn solution from the computer.

The results of this portion of the study do not present any startling new ideas. The findings of this aspect of the problem agree with the classical Hohmann transfer problem which was developed in the 1920's. However, a few interesting observations can be made for the finite burn problem and its possible applications for an IUS mission. First of all, the transfer angle for the finite burn problem at which we have maximum payload is greater than 180°. This fact is evidenced in Figs. 4-1 and 4-2. This result is due to the fact that the transfer angle changes a small amount during the finite burn. The

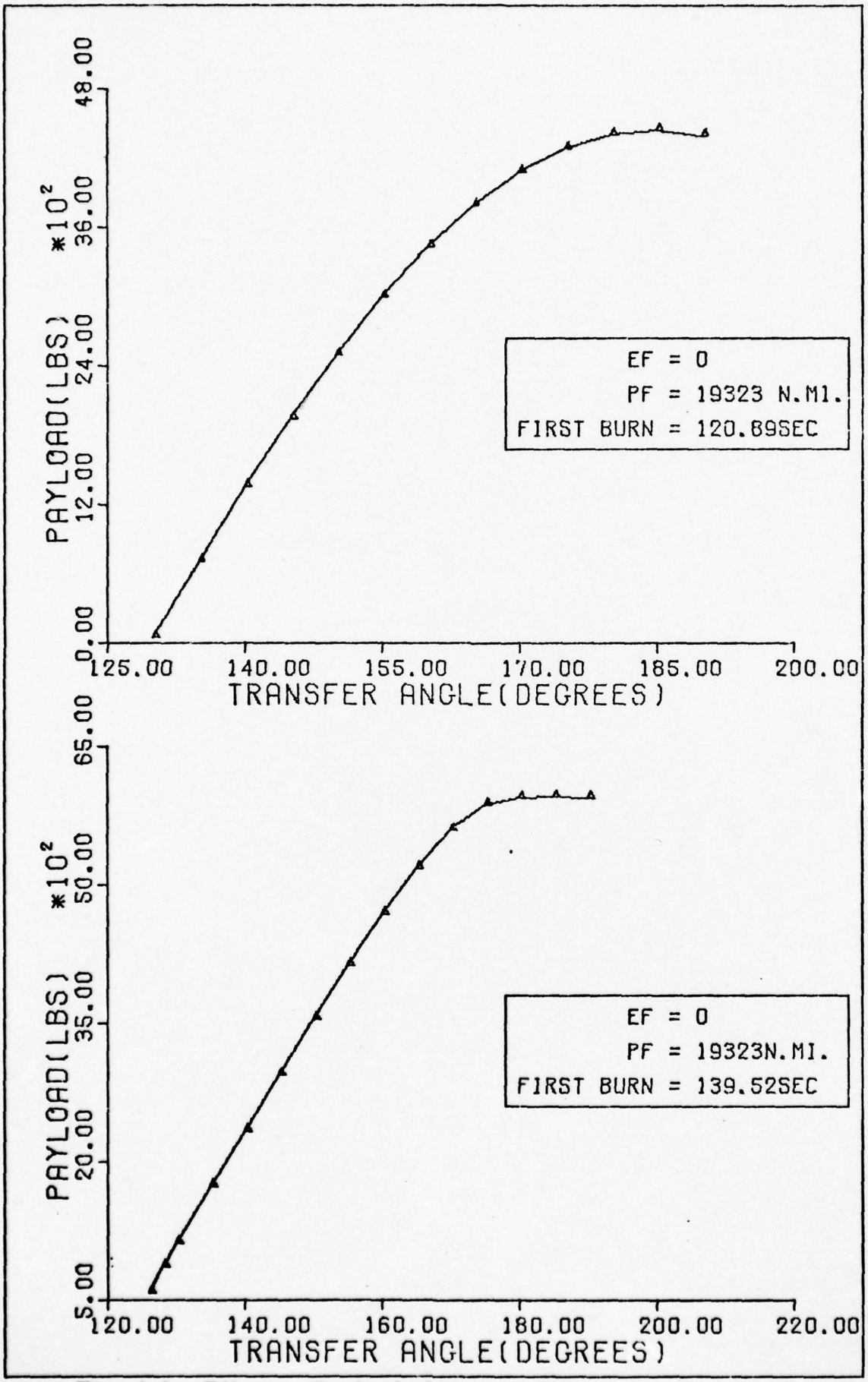

Fig. 4-1. Effect on Payload of Varying Transfer Angle ($e_f = 0$)

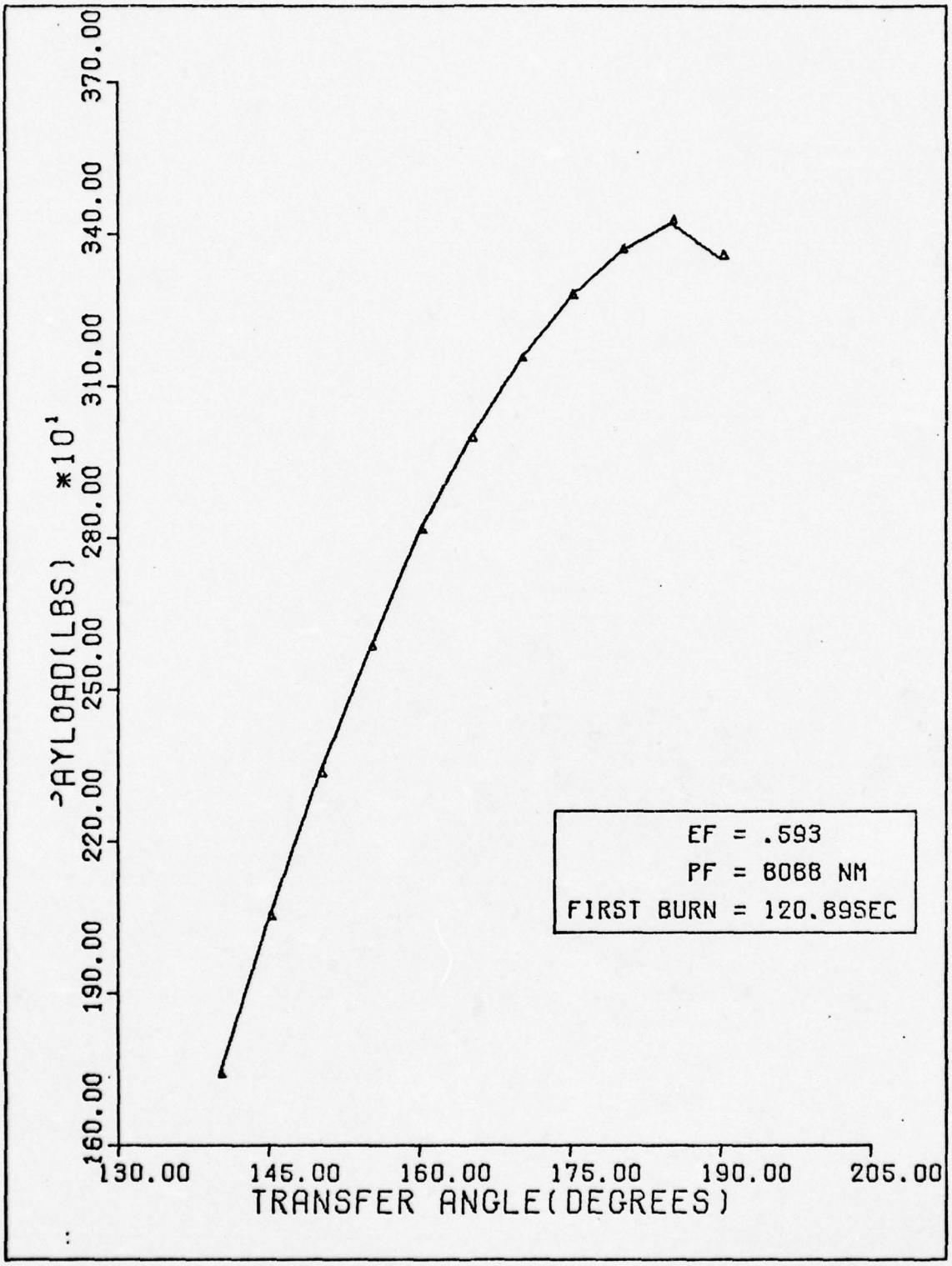

Fig. 4-2. Effect on Payload of Varying Transfer Angle ($e_f \neq 0$)

angle change through the coast period remains approximately 180°. Maximum payload transfers therefore occur at about 185°. This result is consistent throughout the range of transfers examined.

The results of varying the transfer angle seem to imply that this technique may be used as an energy management scheme. For a mission with a payload less than that which can be delivered with a given propellant loading, the present IUS concept is to use a reaction control system to burn excess fuel. An examination of Figs. 4-1 and 4-2 show that such an additional control system may be unnecessary in its application to burn excess fuel. Changing the transfer angle of the mission can achieve the same objective of burning all of the available propellant in an orbital transfer mission.

It is also interesting to examine the range of transfer angles for a given mission. A comparison of the graphs in Fig. 4-1 shows that an increase in first stage propellant loading not only increases the payload which can be delivered, but it also increases the range of transfer angles. The range of transfer angles to the elliptical orbit shown in Fig. 4-2 is smaller than that for transfer to geosynchronous orbit. Figure 4-3 shows the range of transfer angles for a mission to a 14,500 nm orbit. In this case not only has payload capability increased, but the range of transfers has also increased significantly.

Effect of Offloading Fuel. It was mentioned in Chapter I that Boeing's Burner II version of the IUS has the capability to offload

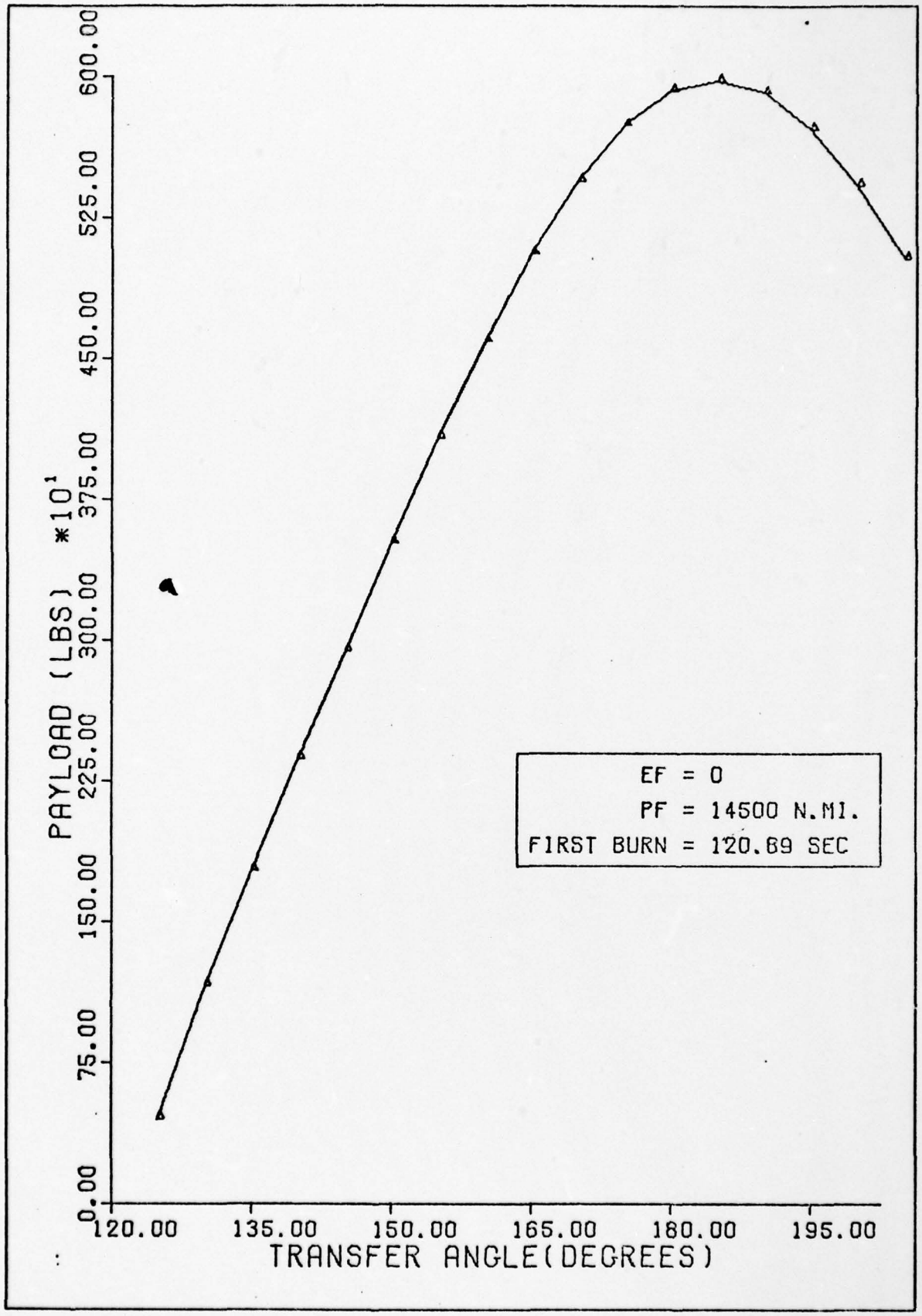

Fig. 4-3. Effect on Payload of Varying Transfer Angle (p_f = 14,500 nm)

fuel. The failure of the thrust termination problem to produce any positive results brought forth the question of offloading. It was originally thought that if thrust termination failed to increase payload that the case three problem with less propellant available should also enable less payload to be delivered to orbit. The results of the investigation appear here in the form of a sizing analysis. For a mission with a specified payload it is possible to examine such an analysis to determine how much propellant is required to achieve the terminal orbit. Economic factors, engineering considerations and other factors can then be considered to determine which sizing is best for a given mission. The sizing analysis was performed for the two primary missions of the IUS with a transfer angle of 180°. The results can be found in Figs. 4-4 and 4-5.

The results of the sizing analysis for the geosynchronous mission show that offloading first stage propellant does not enable more payload to be transported. A decrease in first stage burn will also decrease the available payload. The results for offloading second stage propellant prove to be a bit more interesting. When the maximum available propellant is loaded for the first stage, offloading second stage fuel does not yield any extra payload to orbit. However, as shown in Fig. 4-4, as the first stage fuel is decreased offloading second stage propellant is advantageous in terms of payload capability. With a first stage burn of 132 seconds the maximum payload is delivered with a second burn of 97.5 seconds. Decreasing the second

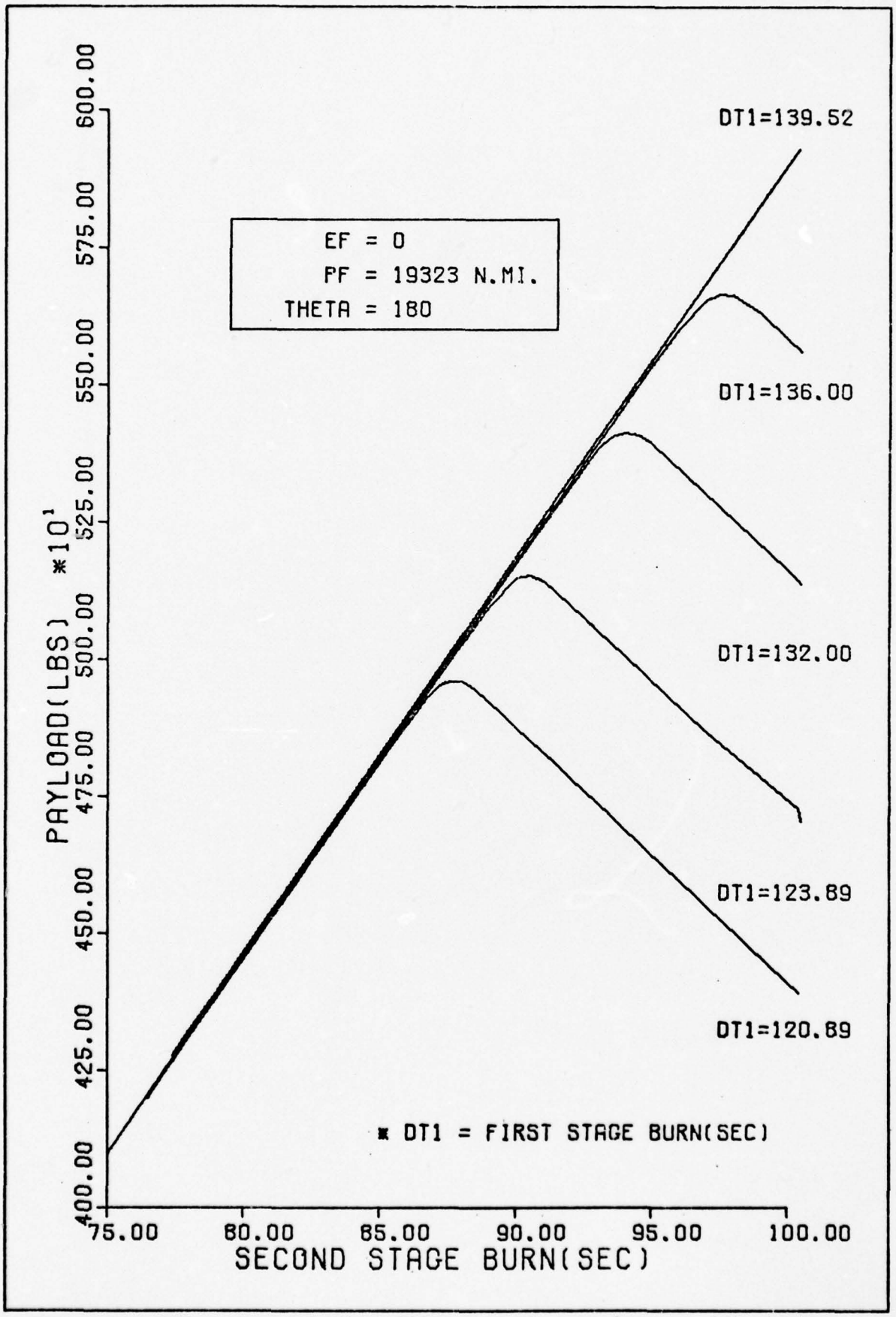

Fig. 4-4. Effect on Payload of Offloading (Geosynchronous Mission)

burn another 1.5 seconds (total offloaded fuel of 206 pounds) would still enable more payload to be delivered than that possible with the full second stage loading. At the lower limit of the first stage propellant loadings (Δt_1 = 120.89 seconds) the maximum payload capability occurs at Δt_2 = 87.6 seconds. Offloading as much as 1029 pounds of second stage fuel for that first stage loading would still enable the same payload to be delivered as that at full second stage loading.

The sizing analysis for the 12 hour mission reveals significantly different findings. The offloading of first stage propellant still does not yield any extra payload. However, offloading second stage fuel increases payload for any first stage loading. It might be mentioned here that the transfer trajectories for the orbital transfer through an angle of 180° are elliptical orbits with relatively high values for eccentricity. It would appear that the velocity change required at the second burn would not be very large for insertion into a similar elliptical orbit. This is exactly the result that was obtained. As shown in Fig. 4-5, the maximum payload is delivered in the neighborhood of a 30 second burn for the second stage motor. For these 12 hour missions 70 percent of the available fuel can be offloaded and still deliver more than 3,000 pounds of additional payload to orbit. Offloading another 700 pounds of fuel would still enable the same amount of payload to be transported to this elliptical orbit.

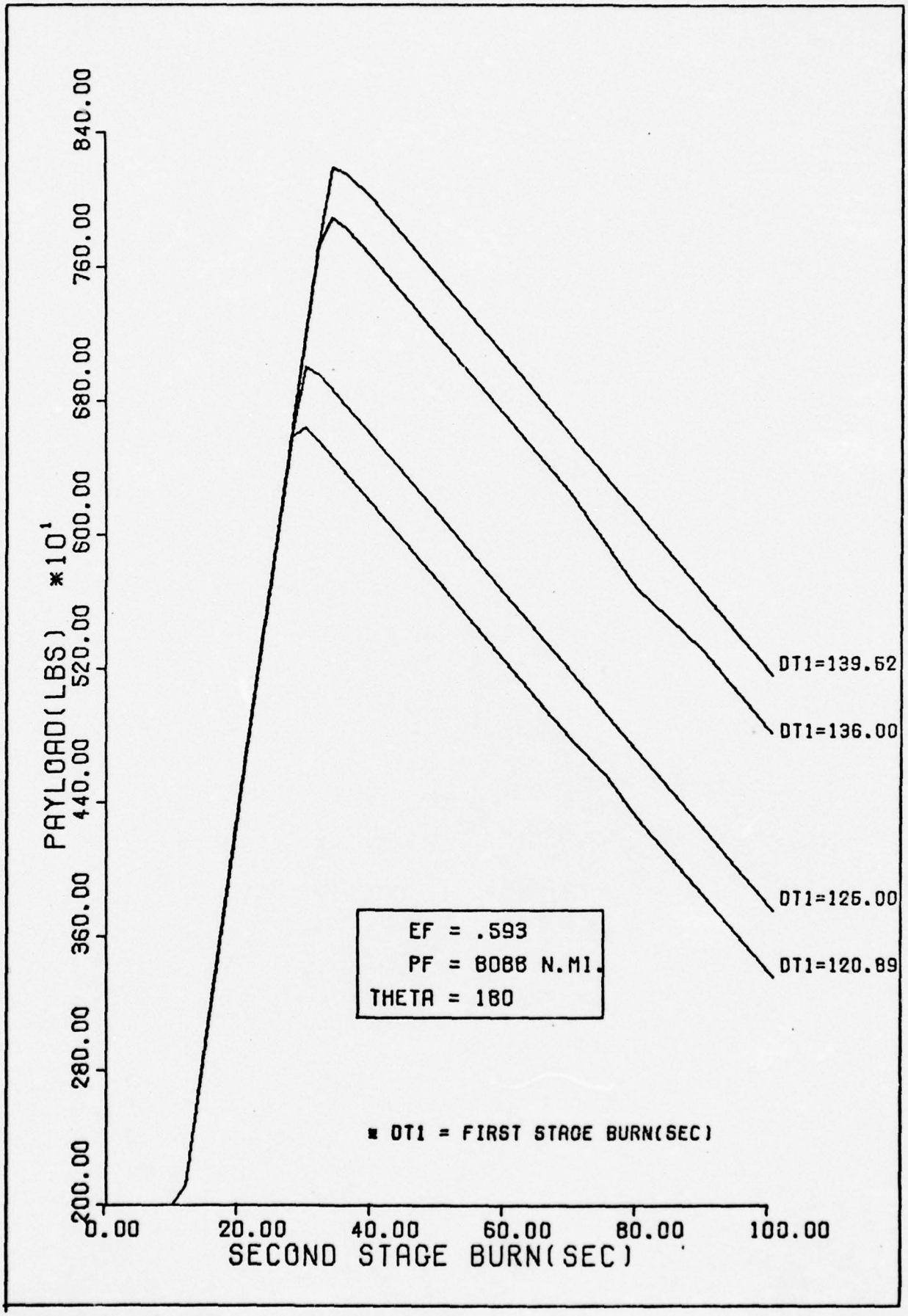

Fig. 4-5. Effect on Payload of Offloading (12 Hour Mission)

Effects of Changing Terminal Orbit Parameters. In addition to the analysis of the three previously mentioned energy management techniques, the maximum payloads that can be delivered to different terminal orbits is also investigated. The semi-latus rectum, p_f, of the final circular orbit was varied and the results appear in Table V. The expected result is that more payload can be delivered to an orbit with a smaller radius.

Table V
Varying p_f of Terminal Circular Orbit ($\theta = 180^o$)

p_f (nm)	5000	10000	13000	16000	19000	19500	21000
Payload (lbs)	8611	6329	6048	5356	4471	4350	4023

Transfers were also made to elliptical terminal orbits. Changing the apogee distance, r_A, and perigee distance, r_p, of the elliptical orbit is described in this problem by eccentricity, e_f, and semi-latus rectum, p_f. The results for the transfers to elliptical orbits for transfer angles of 180^o are presented in Table VI.

Table VI
Maximum Payload Transfers to Elliptical Orbits

	e_f	.218	.0517	.1525	.2445	.456	.593
Terminal	p_f (nm)	19,489.	20,685.	18,965.	15,778.	10,325.	8,088.
Orbit	r_A (nm)	20,000.	22,000.	23,000.	23,000.	22,000.	24,893.
Parameters	r_p (nm)	19,000.	19,500.	16,000.	12,000.	6,000.	3,793.
Payload (lbs)		5,597	5,192	5,017	5,193	5,218	4,724

General Comments. The objective of this optimization as described in Chapter I is to determine the time histories of the controls for the transfer trajectory which yields maximum payload. The mathematical relationships for the controls are given by the optimality condition. Graphs of the time histories of the controls for the two primary IUS missions are given in Figs. 4-6 and 4-7.

Due to the sensitivity of the numerical algorithm to the unknown lagrange multipliers a great deal of computer time was required to obtain solutions for the coplanar problems. The recursive use of the algorithm helped reduce the amount of computer time, but convergence to solutions was still costly. In the transfer to the geosynchronous orbit for example, the full range of transfers required well over 2000 seconds of execution time. This time does not include the time required for convergence to the initial transfers angle in that range. Table VII shows how the unknowns in the problem varied for the different missions.

A pure integration routine, using the values of the unknowns from a successful orbital transfer, was used as a check on the accuracy of the numerical algorithm to search for the correct unknowns. The results of the integration routine show that the desired final conditions are met for the orbital transfer problems. Distance errors between desired and computed values of terminal conditions are on the order of ten feet. Errors in angles are approximately 10^{-7}

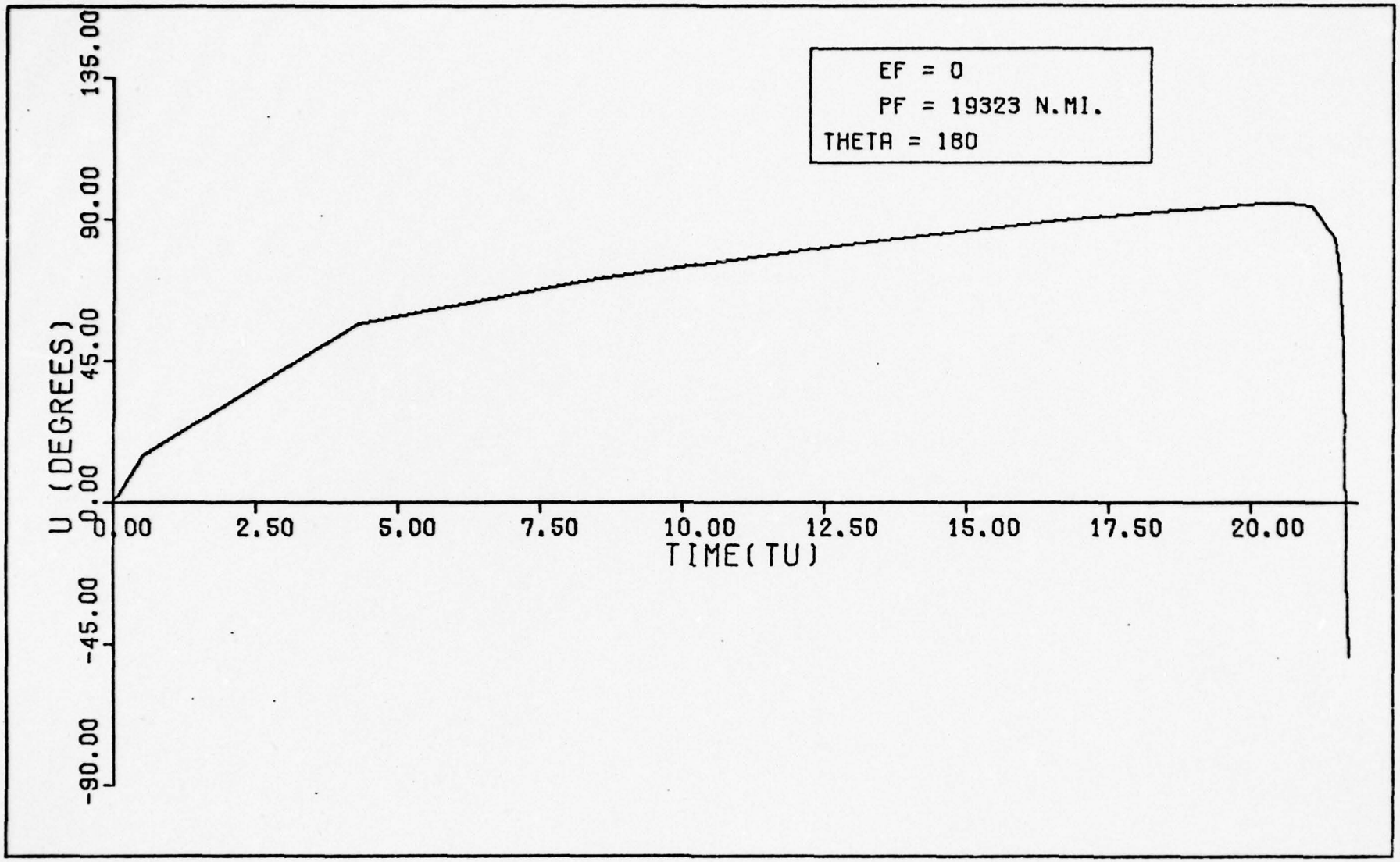

Fig. 4-6. Time History of Control (Geosynchronous Mission)

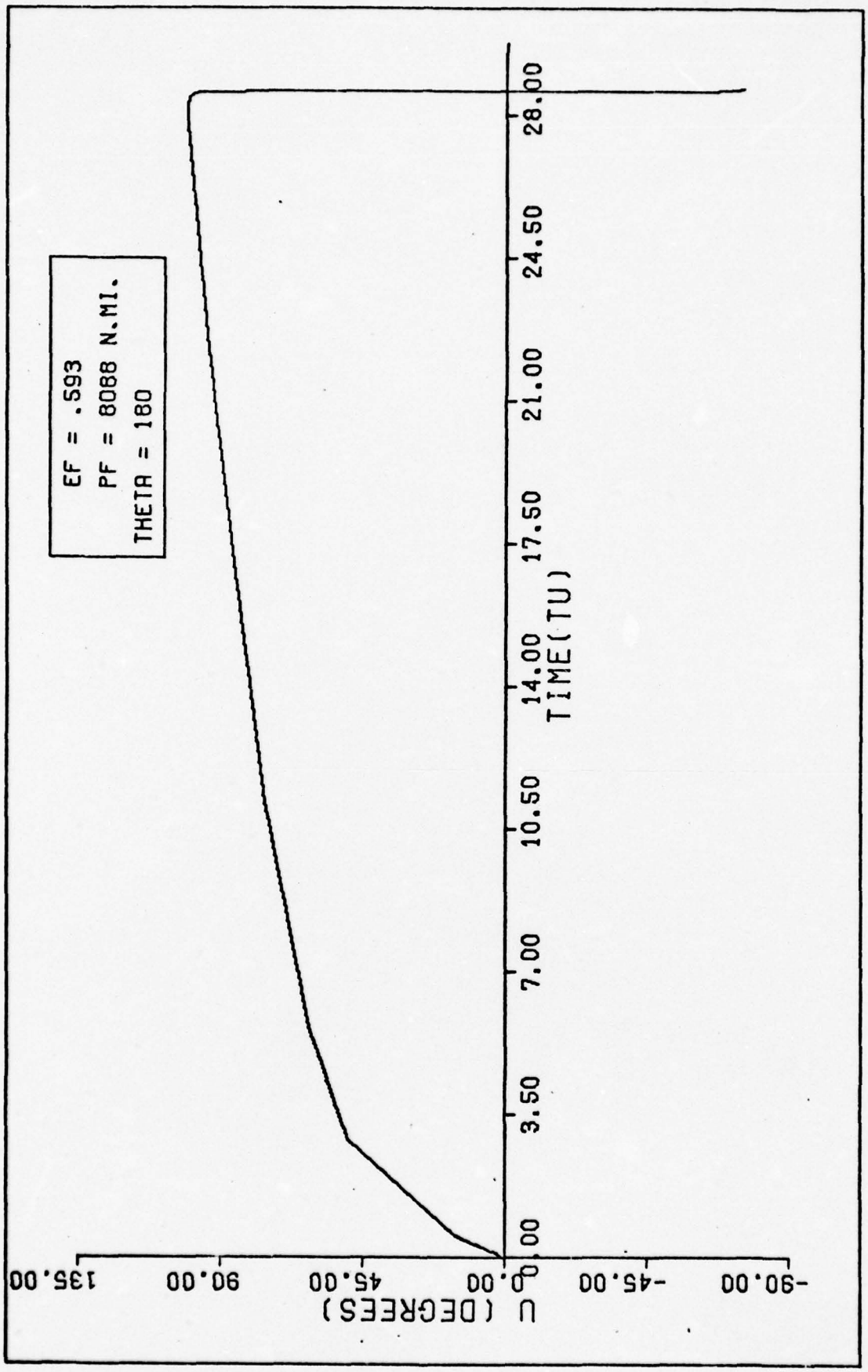

Fig. 4-7. Time History of Control (12 Hour Mission)

Table VII
Coplanar Solutions for Orbital Transfers (Case Three)

Mission \ Unknowns	λ_R	λ_θ	λ_{V_R}	λ_θ	$m(t_o)$ (lbs)	t_2 (TU)
Geosynchronous						
$\theta = 185$	.09145	-.00027	.00849	-.37002	30,227	23.617
$\theta = 180$	.09097	.00571	-.00619	-.37012	30,189	21.610
$\theta = 175$	.08896	.01163	-.02070	-.36623	30,067	19.884
$\theta = 170$	.08547	.01739	-.03470	-.35843	29,863	18.381
$\theta = 165$	.08059	.02293	-.04792	-.34692	29,579	17.060
12 Hour Mission						
$\theta = 185$	.08331	.00033	.00795	-.32987	29,216	31.300
$\theta = 180$	.08270	.00531	-.00538	-.32920	29,159	28.528
$\theta = 175$	.08107	.01091	-.01859	-.32670	29,068	25.819
$\theta = 170$	.07843	.01642	-.03155	-.32238	28,944	23.215
$\theta = 165$	.07480	.02182	-.04416	-.31629	28,787	20.757

degrees. Velocity errors are on the order of 10^{-3} feet per second. Accuracy even better than that obtained is possible, to a certain extent, by demanding more accuracy from the search routine, NS01A.

Results of the Noncoplanar Transfers

It was noted in the previous section that the numerical algorithm was very sensitive to errors in the unknowns and that convergence was often difficult to obtain. This problem became even more pronounced in the noncoplanar transfer due to the additional states and lagrange multipliers.

Cross Check of Noncoplanar and Coplanar Transfers. The first task that was attempted for the noncoplanar transfer was a check on the claim of Appendix B. That claim was that the noncoplanar transfer state equations could be used for a coplanar problem by simply setting the noncoplanar inclination angle equal to zero. The resulting comparisons of the use of two different sets of equations for the same problem appear in Table VIII. It can be seen that both approaches give the same maximum payload to within one tenth of a pound. This holds true for both first stage propellant loadings.

Effect of Changing Inclination Angle. Due to the extreme sensitivity to variations in the unknowns for the noncoplanar problem, the recursive use of the algorithm was once again required. The inclination angle was incremented by one fourth of a degree for each

successive problem. Approximately 1000 seconds of computer time was still required to achieve the necessary convergence. Table IX shows how the unknowns changed by incrementing the inclination angle.

The trends shown in Table IX continue as the inclination angle is increased. It therefore appears that it would not be possible to deliver a payload beyond a five degree inclination angle. These results are not consistent with the claims of Ref 4, that payloads of more than 3000 pounds can be delivered through an inclination angle of 28.5°. The numerical algorithm was also checked for a first burn of 139.52 seconds. An inclination angle of 10° and transfer angle of 140° were used for the transfer. According to the solutions from the algorithm only 414 pounds of payload can be delivered. This is once again far below the stated payload capability given in Ref 4. The next step taken was to change the transfer angle to determine at what angle the maximum payload could be delivered. Changing the transfer angle to 145° for $i = 10^{\circ}$ reduced the payload to 215 pounds. Similar results were obtained when the transfer angle was incremented for $i = 1^{\circ}$. This result is in direct contradiction of the results of the Hohmann problem. Even though a noncoplanar transfer is being accomplished increasing the transfer angle should result in increased payload capability. Various other initial guesses for the unknowns failed to yield convergence to the noncoplanar transfer.

Table VIII
Payload Check of Coplanar and Noncoplanar (i=0) Problems

Mission / Problem	Δt_1=120.89 sec θ = 170	Δt_1=120.89 sec θ = 175	Δt_1=120.89 sec θ = 180	Δt_1=139.52 sec θ = 165	Δt_1=139.52 sec θ = 170
Coplanar Payload (lbs)	4065.9154	4269.9729	4391.8041	5165.7151	5578.1003
Noncoplanar Payload (i=0) (lbs)	4065.7758	4269.8921	4391.8338	5165.6073	5578.2068

Table IX
Effect of Inclination Angle on Payload (Δt_1=120.89)

Inclination Angle (i) / Unknown	i = .5	i = 1.0	i = 1.5
λ_R	-.25801	-.24083	-.21683
λ_θ	.01211	-.00362	-.02618
λ_ϕ	-.17097	-.32619	-.44273
λ_{V_R}	-.03454	-.03310	-.03054
λ_{V_θ}	-.36318	-.33826	-.30365
λ_{V_ϕ}	.03127	.05985	.08178
$m(t_o)$ (lbs)	29,747.0	29,395.0	28,845.0
t_2 (TU)	18.41236	18.43926	18.43366
payload (lbs)	3,949.76	3,598.17	3,047.85

Since the results indicate a non-optimal solution for the non-coplanar transfer an impulsive approximation of a 1^{o} plane change was examined to determine how much the payload would be affected by such a change. The 1^{o} plane change for a Hohmann transfer to a geosynchronous orbit for the vehicle parameters of this problem cost 282 lbs of payload. This is far below the decrease in payload for the same plane change as indicated by the computer results. It thus appears that NS01A has converged to a non-optimal solution.

Use of Integration Scheme to Check Noncoplanar Problem. In order to determine just where the search routine was placing the IUS for a payload that is obviously non-optimum, an integration scheme was employed. The method is the same as that used in the coplanar problem. The unknowns obtained from a successful solution in terms of convergence accuracy were input to an integration routine. The desired and actual values of the terminal conditions were then compared. The results, which appear in Table X, indicate that the unknowns are correct in terms of getting the vehicle to the proper terminal conditions.

Table X
Results of Integration Scheme (i=10, θ'=140, Δt_1=139.52)

State	Computed Value	Desired Value	Error (Magnitude)
r	6.610734611704 DU	6.610734442127 DU	4.18 ft.
θ	139.5675381°	139.5675389°	8.0×10^{-7} deg.
ϕ	82.3557286°	82.35572992°	1.32×10^{-6} deg.
V_R	5.84655×10^{-7} DU/TU	0.00	.012968 ft/sec
V_θ	.3899247944172 DU/TU	.3899240926573 DU/TU	.018155 ft/sec
V_ϕ	-.04380487048311 DU/TU	-.04380155563068 DU/TU	.08559 ft/sec

Similar results were obtained when the integration scheme was used to test the accuracy for the problem with i = 1.

V. Conclusions

Three energy management techniques have been applied to the maximum payload orbital transfers problems.

The coplanar results for these energy management techniques indicate that optimal solutions for thrust termination problems cannot be found using the numerical algorithm of this study. However, the analytic argument presented indicates that thrust termination does not increase payload capability of the IUS.

On the other hand, varying the transfer angle and offloading fuel are two possibilities for managing IUS propellant. Variation of the transfer angle can achieve the same objective as a reaction control system that is used to burn excess fuel. The sizing analysis provided by investigating the offloading problem enables one to choose the best of a variety of propellant loadings for a mission with a specified payload.

Although solutions were not obtained for the noncoplanar problem it is assumed that the coplanar results regarding the energy management techniques can be extended to the noncoplanar problem. That is, of the three energy management techniques investigated, only the thrust termination problem would not yield positive results.

Convergence to solutions was difficult with the non-linear equation solver, NS01A, due to the sensitivity of the problem to such factors as the costates and switching functions. A great deal of care in scaling the problem and choosing the best step length for NS01A still left the fact that a great deal of computer time was required to obtain solutions.

Bibliography

1. Anderson, Gerald M. Introduction to Optimization Techniques. Unpublished lecture notes. Wright-Patterson AFB: Air Force Institute of Technology, 1976.

2. Anderson, Gerald M., and Eugene A. Smith. "A Combined Gradient/Neighboring External Algorithm for the Calculation of Optimal Transfer Trajectories between Noncoplanar Orbits Using a Constant Low Thrust Rocket," Journal of the Astronautical Sciences, Vol. XXIII, No. 3: 225-239 (July-September 1975).

3. Bate, Roger R., et al. Fundamentals of Astrodynamics. New York: Dover Publications, Inc., 1971.

4. Boeing Aerospace Company. Burner II Interim Upper Stage Study, Vol. II, D 180-18425-25. Seattle: Boeing Aerospace Company, 1975.

5. Bryson, Arthur E., and Vu-Chi Ho. Applied Optimal Control. New York: John Wiley and Sons, 1975.

6. Johnson, Raymond P. Time-Optimal Rendezvous for an Upper Stage Vehicle of the Space Transportation System. Paper, AIAA/AAS Astronautical Conference, San Diego, California, 1976.

7. Powell, M. J. D. "A Fortran Subroutine for Solving Systems of Nonlinear Algebraic Equations." Numerical Methods for Nonlinear Algebraic Equations, edited by Rabinowitz, P., et al. New York: Gordon and Breach Science Publishers, 1972.

Appendix A

Coplanar Equations of Motion and Boundary Conditions

The coplanar orbital transfer as formulated here is just a special case of a noncoplanar transfer for which the inclination angle between the initial and final orbits is zero. The equations of motion derived in this appendix provide state equations which differ from those of the noncoplanar problem and thus serve as a check for one case of the more difficult noncoplanar transfer.

Equations of Motion

The motion of a vehicle that is subject only to gravitational and propulsive forces can be described by the following differential equation:

$$\ddot{\underline{r}} = \underline{G}\,(r, t) + \frac{\underline{F}(t)}{M(t)} \qquad \text{(A-1)}$$

where

$\underline{r}$ is the position vector of the vehicle

t represents time

$\underline{G}(r, t)$ is the force due to gravity

$\underline{F}(t)$ is the force due to thrust

$M(t)$ is the mass of the vehicle

and $(\dot{})$ indicate differentiation with respect to time

The assumptions of Chapter I dictate that the gravitational attraction is an inverse-square central force, therefore

$$\underline{G}(r, t) = -\frac{\mu \underline{r}}{r^3} \tag{A-2}$$

where μ is the gravitational parameter and r is the magnitude of the position vector. Restricting thrust to lie within a plane enables one to write $\underline{F}(t)$ in terms of thrust magnitude, T, and steering angle, α, as shown in Fig. A-1.

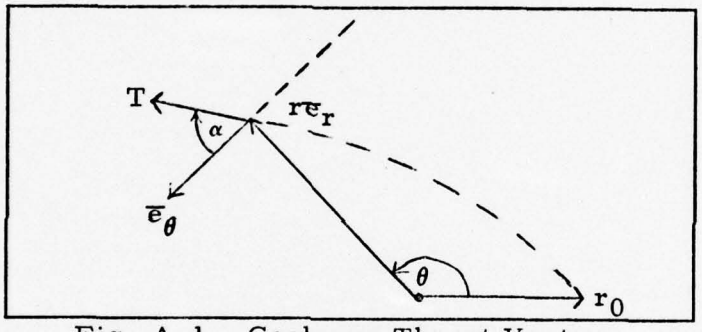

Fig. A-1. Coplanar Thrust Vector

The expression for acceleration of the vehicle in terms of radial, $\bar{e}_r$, and tangential, $\bar{e}_\theta$, components becomes:

$$\ddot{\underline{r}} = \left(-\frac{\mu}{r^2} + \frac{T}{m} \cos \alpha \right) \bar{e}_r + \frac{T}{m} \sin \alpha \bar{e}_\theta \tag{A-3}$$

Another expression for acceleration can be obtained by twice differentiating the position vector, $r\bar{e}r$, of the vehicle with respect to time. The angular velocity of the vehicle needed for the differentiation is:

$$\underline{\omega} = \dot{\theta}\, \bar{e}_z \tag{A-4}$$

where θ is the angle between $\underline{r}(t)$ and $\underline{r}\,(t + \Delta t)$, and $\bar{e}_z$ is the unit vector normal to the plane of motion. The well-known result of this operation is

$$\ddot{\underline{r}} = (\ddot{r} - r\dot{\theta}^2)\,\bar{e}_r + (2\dot{r}\dot{\theta} + r\ddot{\theta})\bar{e}_\theta \qquad \text{(A-5)}$$

Equating components of the two acceleration equations yields the following equations:

$$\ddot{r} - r\dot{\theta}^2 = -\frac{\mu}{r^2} + \frac{T}{m}\sin\alpha$$

$$2\dot{r}\dot{\theta} + r\ddot{\theta} = \frac{T}{m}\cos\alpha \qquad \text{(A-6)}$$

Three states that may be used in this problem are position, r, central angle, θ, and radial velocity, V_R. Two of the differential equations are therefore:

$$\dot{r} = V_R \qquad \text{(A-7)}$$

$$\dot{\theta} = \frac{V_\theta}{r} \qquad \text{(A-8)}$$

where V_θ is tangential velocity. Substituting these equations plus the time derivatives of Eq (A-8) into Eqs (A-6) gives the following relationships:

$$\dot{V}_R = \frac{V_\theta^2}{r} - \frac{\mu}{r^2} + \frac{T}{m}\sin\alpha \qquad \text{(A-9)}$$

$$\dot{V}_\theta = \frac{T}{m} \cos \alpha - \frac{V_R V_\theta}{r} \qquad \text{(A-10)}$$

The knowledge that angular momentum is constant during coast phases of a trajectory provides the motivation for its use as a state. The equation for angular momentum is:

$$\underline{h} = \underline{r} \times \underline{V} \qquad \text{(A-11)}$$

where $\underline{h}$ is angular momentum and $\underline{V}$ is the velocity vector. Angular momentum for coplanar motion is therefore

$$h = rV_\theta \qquad \text{(A-12)}$$

Substitution of Eq (A-12) into Eq (A-9) and Eq (A-10) gives the final form for these state equations.

Since mass varies with time during thrusting periods, it can be described by a differential equation in terms of thrust and effective exhaust velocity, C.

$$\dot{m} = -\frac{T}{C} \qquad \text{(A-13)}$$

The state equations for coplanar transfer therefore are:

$$\begin{aligned} \dot{r} &= V_R \\ \dot{\theta} &= \frac{h}{r^2} \\ \dot{V}_R &= \frac{h^2}{r^3} - \frac{\mu}{r^2} + \frac{T}{m} \sin \alpha \end{aligned} \qquad \text{(A-14)}$$

$$\dot{h} = \frac{Tr}{m} \cos \alpha$$

$$\dot{m} = -\frac{T}{C}$$

Boundary Conditions

The formulation of the boundary value problem requires that the values of the states at the endpoints be determine a priori or by the numerical algorithm. The initial values of four of the states are specified by the parameters of the parking orbit from which the mission begins. Those conditions are:

$$\begin{aligned} r(0) &= r_o \\ \theta(0) &= 0 \\ V_{R_o} &= 0 \\ h(0) &= \sqrt{\mu r_o} \end{aligned} \qquad \text{(A-15)}$$

The initial value of the mass state variable is unknown in that the algorithm seeks the maximum initial mass for which a transfer can be made. An initial guess at this value was determined from the specifications of the Boeing Burner II vehicle.

It is assumed that the final orbit parameters and the orbit transfer angle for a mission are determined a priori. The desired final orbit is prescribed by the semi-latus rectum, p_f, and eccentricity, e_f. For a given transfer angle, θ_f, the final radius is given by:

$$r_f = \frac{p_f}{1 + e_f \cos \theta_f} \qquad \text{(A-16)}$$

The final radial velocity in terms of the specified parameters is:

$$V_{r_f} = \sqrt{\frac{\mu}{p_f}}\ e_f \sin \theta_f \qquad \text{(A-17)}$$

Final angular momentum is given by:

$$h_f = \sqrt{\mu p_f} \qquad \text{(A-18)}$$

The final mass is not required for solution of the MPBVP as shown in Chapter II.

Appendix B

Noncoplanar Equations of Motion and Boundary Conditions

The equations derived in this appendix can be used for either a noncoplanar or coplanar transfer by adjusting the inclination angle between the initial and final orbits. Much of the work in deriving the state equations and boundary conditions for this problem can be found in References 2 and 6 . The general case of the noncoplanar transfer can be seen in Fig. B-1.

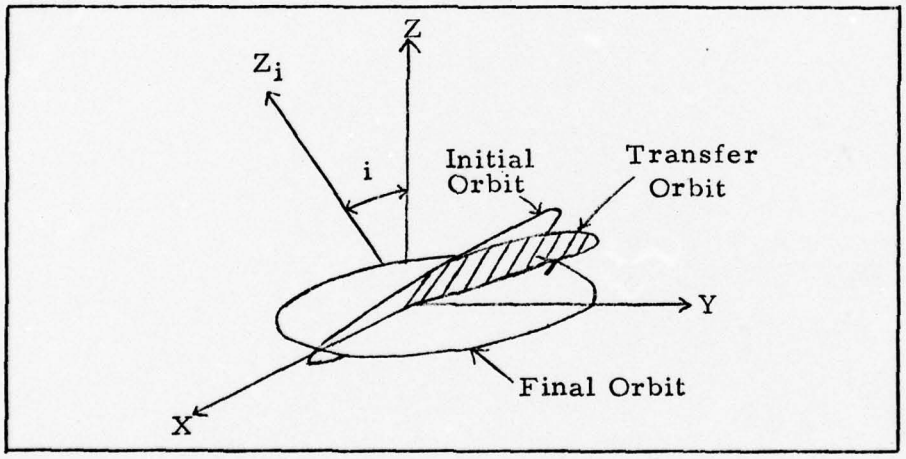

Fig. B-1. Noncoplanar Transfer

Equations of Motion

As in the coplanar case the motion of the vehicle is determined by Eq (A-1) which is repeated here:

$$\ddot{\underline{r}} = \underline{G}(r, t) + \frac{\underline{F}(t)}{M(t)} \qquad \text{(B-1)}$$

The gravitational force, $\underline{G}(r, t)$ is written as in Appendix A, but the propulsive force, $\underline{F}(t)$, is written in terms of the $r\text{-}\phi\text{-}\theta$ spherical coordinate system. Figure B-2 shows the applied thrust vector F(t) in the $r\text{-}\phi\text{-}\theta$ frame.

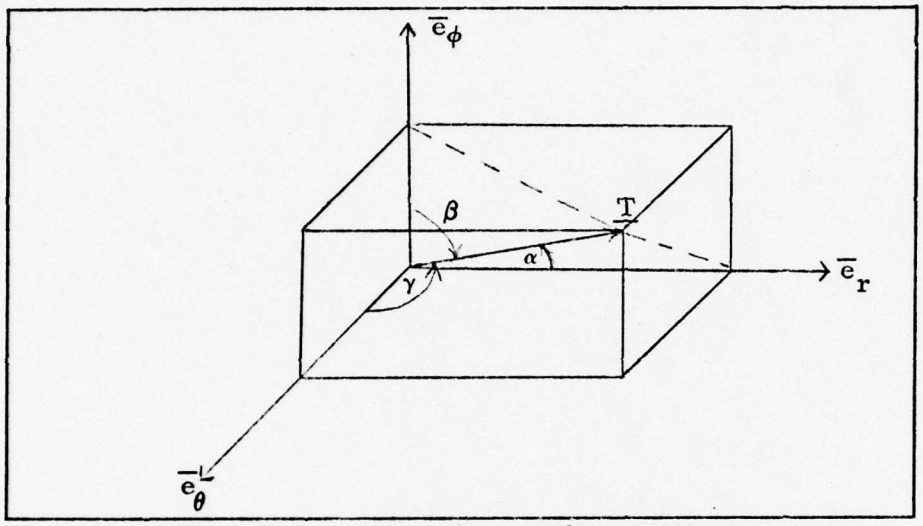

Fig. B-2. Noncoplanar Thrust Vector

The equation of motion in spherical coordinates is therefore written as:

$$\ddot{\underline{r}} = \left(-\frac{\mu}{r^2} + \frac{T\ell_1}{m} \right) \bar{e}_r + \frac{T\ell_2}{m}\, \bar{e}_\phi + \frac{T\ell_3}{m}\, e_\theta \qquad \text{(B-2)}$$

where

μ is the gravitational parameter

r is the magnitude of the radius vector

T is thrust magnitude

m is vehicle mass

and ℓ_1, ℓ_2, ℓ_3 are the direction cosines associated with α, β and γ respectively.

Another expression for the acceleration of the vehicle is sought by differentiating the position vector twice with respect to time. The position vector is:

$$\underline{r} = r\bar{e}_r \tag{B-3}$$

The relationship of the r-ϕ-θ frame to a frame fixed in the orbital plane can be seen in Fig. B-3.

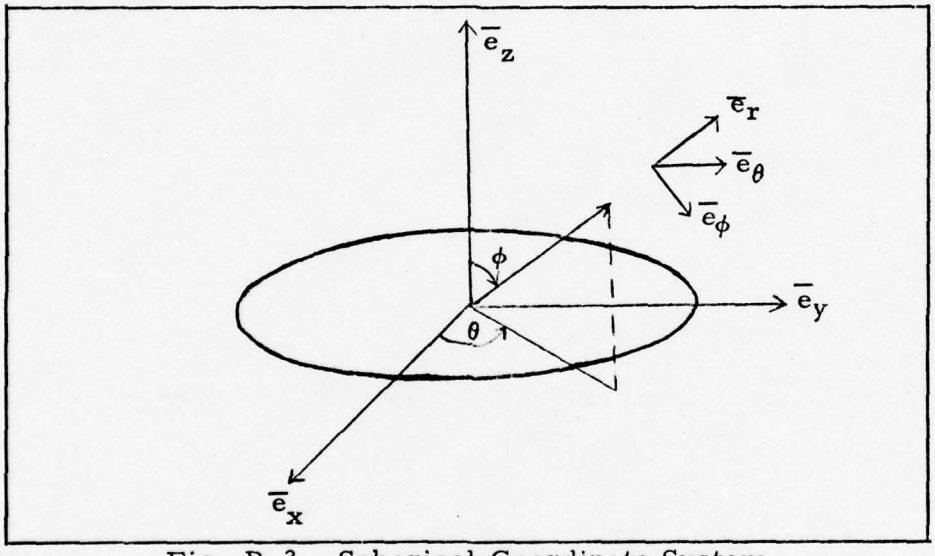

Fig. B-3. Spherical Coordinate System

The angular velocity of the spherical coordinate system with respect to the fixed reference frame is:

$$\omega = \dot{\theta} \cos \phi \, \bar{e}_r - \dot{\theta} \sin \phi \, \bar{e}_\phi + \dot{\phi}\bar{e}_\theta \tag{B-4}$$

Applying this expression for angular velocity in the differentiation of the position vector yields the following expression for vehicle acceleration:

$$\ddot{\underline{r}} = (\ddot{r} - r\dot{\theta}^2 \sin^2\phi - r\dot{\phi}^2)\,\bar{e}_r$$

$$+ (2\dot{r}\dot{\phi} - r\dot{\theta}^2 \sin\phi\cos\phi + r\ddot{\phi})\,\bar{e}_\phi \qquad \text{(B-5)}$$

$$+ (2\dot{r}\dot{\theta}\sin\phi + r\ddot{\theta}\sin\phi + 2r\dot{\theta}\dot{\phi}\cos\phi)\,\bar{e}_\theta$$

Having found this second equation for acceleration it is now possible to determine the state equations. Differential state equations in r, θ, and ϕ are defined as:

$$\dot{r} = V_R$$

$$\dot{\theta} = \frac{V_\theta}{r} \qquad \text{(B-6)}$$

$$\dot{\phi} = \frac{V_\varphi}{r}$$

Equating like components of Eq (B-2) and Eq (B-5) yields the following state equations for V_R, V_θ and V_ϕ:

$$\dot{V}_R = \frac{V_\theta^2}{r}\sin^2\phi + \frac{V_\phi^2}{r} - \frac{\mu}{r^2} + \frac{T_{l_1}}{m}$$

$$\dot{V}_\phi = -\frac{V_R V_\phi}{r} + \frac{V_\theta^2}{r}\sin\phi\cos\phi + \frac{T_{l_2}}{m} \qquad \text{(B-7)}$$

$$\dot{V}_\theta = -\frac{V_R V_\theta}{r} - \frac{2V_\theta V_\phi \cos\phi}{r\sin\phi} + \frac{T_{l_3}}{m\sin\phi}$$

An additional differential equation for the time rate of change of mass is:

$$\dot{m} = -\frac{T}{C} \qquad \text{(B-8)}$$

where C is the effective exhaust velocity.

The seven state equations required for the noncoplanar transfer are given by Eqs (B-6), (B-7), and (B-8).

Boundary Conditions

The values of the states at the boundaries must be given or the algorithm must seek their value to give a solution to the boundary value problem. Initial values which are prescribed as in Appendix A are

$$\begin{aligned} r(0) &= r_o \\ \theta(0) &= 0 \\ V_R(0) &= 0 \end{aligned} \tag{B-9}$$

The initial orbit is assumed to be in the $\bar{e}_x$, $\bar{e}_y$ plane as shown in Fig. B-2. The angle ϕ is therefore given by

$$\phi(0) = 90^o \tag{B-10}$$

This assumption gives the value of V in the initial orbit as:

$$V_\phi(0) = 0 \tag{B-11}$$

The tangential velocity of a satellite in circular orbit is given by:

$$V_\theta(0) = \sqrt{\frac{\mu}{r_o}} \tag{B-12}$$

The algorithm described in Chapter II seeks a value for the initial mass of the vehicle.

The desired final conditions are determined from algebraic relationships as in Appendix A. The final eccentricity, e_f, semi-latus rectum, p_f, and desired transfer angle in the plane of the final orbit, θ'_f, are given. The final radius is therefore given as:

$$r_f = \frac{pf}{1 + e_f \cos \theta'_f} \tag{B-13}$$

In order to determine θ_f and ϕ_f in the initial orbit plane we must use spherical trigonometry. The spherical triangle which describes the relationship between the initial and final orbit is shown in Fig. B-4.

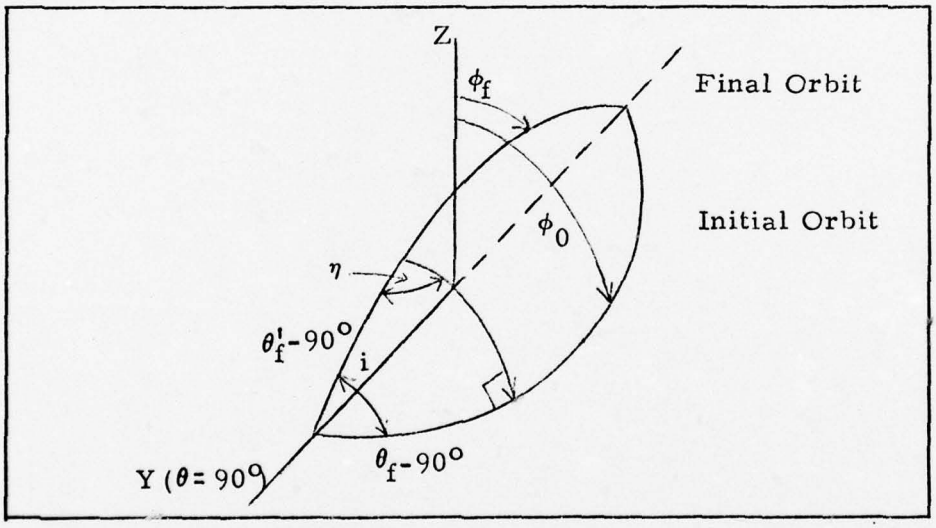

Fig. B-4. Spherical Angles for Noncoplanar Problem

Napier's rules for right spherical triangles gives the following relationships:

$$\begin{aligned} \sin(\phi_0 - \phi_f) &= \cos(90 - i) \cos(180 - \theta') \\ \sin(\theta - 90) &= \tan(\phi_0 - \phi_f) \tan(90 - i) \end{aligned} \tag{B-14}$$

Using reduction formulae and knowledge of ϕ_0 we can obtain the required relationships:

$$\phi_f = 90 - \sin^{-1}(-\sin i \cos \theta') \tag{B-15}$$

$$\theta_f = \cos^{-1}[\tan(90-\phi_f)\cot i] \tag{B-16}$$

It is now required to derive expressions for the velocities at the final time. The expression for radial velocity shown in Appendix A applies in the noncoplanar case as well:

$$V_{R_f} = \frac{e_f h_f \sin \theta'_f}{p_f} \tag{B-17}$$

Where h_f is the angular momentum of the final orbit. Relationships for V_ϕ and V_θ can be found by examining expressions for angular momentum. By definition

$$\underline{h} = \underline{r} \times \underline{v} \tag{B-18}$$

which in spherical coordinates is:

$$\underline{h} = r V_\phi e_\theta - r V_\theta \sin\phi e_\phi \tag{B-19}$$

Another expression for angular momentum in the terminal orbit is:

$$\underline{h} = h_f \sin i \, \bar{e}_x + h_f \cos i \, \bar{e}_z \tag{B-20}$$

Eq (B-19) and (B-20) can be equated after the coordinate transformation between the x-y-z frame and r-ϕ-θ frame is made. The transformation matrix given by three successive rotations of the spherical

coordinate system through angles of $(90^{o}-\phi)$, θ, and 90^{o} will give the appropriate expressions for $\bar{e}_x$ and $\bar{e}_z$ in Eq (B-20).

$$\bar{e}_x = \cos\theta \sin\phi\, \bar{e}_r + \cos\theta \cos\phi\, \bar{e}_\phi - \sin\theta\, \bar{e}_\theta \qquad \text{(B-21)}$$

$$\bar{e}_z = \cos\phi\, \bar{e}_r - \sin\phi\, \bar{e}_\phi$$

The expressions that result from substituting Eq (B-21) into Eq (B-20) and equating that to Eq (B-19) is:

$$V_\theta = \frac{h_f}{r_r} (\cos i - \sin i \cos\theta_f \cot\phi_f) \qquad \text{(B-22)}$$

$$V_\phi = -\frac{h_f}{r_f} \sin i \sin\theta$$

Eqs (B-13), (B-15), (B-16), (B-17), and (B-22) are the expressions required to give the boundary conditions at the final time.

Appendix C

Derivation of Necessary Conditions

The presence of constraints on problem variables, i.e. mass and time, at intermediate points (first stage cutoff, staging, and second stage ignition) leads to a set of unique necessary conditions for this multipoint boundary value problem (MPBVP). Those conditions, as derived by the use of the Calculus of Variations, are presented in this chapter for a complete understanding of the problem formulation.

Cost Function

The problem of maximizing the payload of a space vehicle with a fixed amount of fuel and structure drop-off weight is interpreted as minimizing the negative of the initial mass. With that interpretation the performance index, or cost function, as described in Ref 5 is:

$$J = - m(t_o) \tag{C-1}$$

where m is the mass state variable and t_o is the initial time. The intermediate boundary conditions that must be met in the problem appear as inequality constraints on mass and thrusting times for each of the two stages. Those conditions are:

$$C - [m(t_s^-) - m(t_s^+)] \geq 0 \tag{C-2}$$

$$t_{1max} - t_1 \geq 0 \tag{C-3}$$

$$t_{2max} - (t_f - t_2) \geq 0 \tag{C-4}$$

where C is the maximum allowable change in mass at staging

$m(t_s^-)$ is the mass just prior to staging

$m(t_s^+)$ is the mass just after staging

t_{1max} is the maximum allowable time for first stage burning

t_1 is the first stage cutoff time

t_{2max} is the maximum allowable time for second stage burning

t_2 is the second stage ignition time

t_f is the time the orbit transfer is complete.

The end conditions which must be met are the desired final values of the states (except mass) which are specified a priori. They are denoted by the vector:

$$\underline{\psi}\,[\underline{x}(t_f)] \tag{C-5}$$

where x represents the state variables. The cost function is minimized subject to the differential equations in the state variables:

$$f(x, u, t) = \dot{x} \tag{C-6}$$

where u is the control variable.

An augmented cost function is formed by adjoining the above mentioned constraints to the original cost function by the use of

lagrange multipliers. Due to the possibility of discontinuities in the problem the differential constraints are separated into four intervals in the augmented cost function. The cost function is now stated as:

$$\begin{aligned}\tilde{J} = &- m(t_o) + \vartheta^T \psi [x(t_f)] + \pi_1 [C - m(t_s^-) + m(t_s^+)] \\ &+ \pi_2 [t_{1max} - t_1] + \pi_3 [t_{2max} - t_f + t_2] + \\ &+ \int_{t_o}^{t_1^-} \lambda^T (f_1 - \dot{x})\, dt + \int_{t_1^+}^{t_s^-} \lambda^T (f_2 - \dot{x})\, dt \\ &+ \int_{t_s^+}^{t_2^-} \lambda^T (f_3 - \dot{x})\, dt + \int_{t_2^+}^{t_f} \lambda^T (f_4 - \dot{x})\, dt\end{aligned} \tag{C-7}$$

where ϑ, λ, and π are lagrange multipliers, and f_i, $i = I, \ldots 4$ are the state equations during the consecutive phases of the problem.

The optimization problem defined by this performance index can be reduced to an MPBVP by applying the necessary conditions of optimality which will be derived from the classical Calculus of Variations.

Necessary Conditions

The necessary conditions are derived by performing a multivariable Taylor series expansion of $\tilde{J}$ about a nominal trajectory. Higher order terms are neglected and the first variation is set to zero following the general method in Ref 1. Variations of the form:

$$x(t) = x^*(t) + \delta x(t)$$

$$u(t) = u^*(t) + \delta u(t) \qquad \text{(C-8)}$$

$$\dot{x}(t) = \dot{x}^*(t) + \delta \dot{x}(t)$$

where $(\ )^*$ indicates a nominal point, give the following result after a Taylor Series expansion and integration by parts of the appropriate terms:

$$\delta \tilde{J} = [\phi_x + \lambda^T(t_o)]\, dx\,(t_o) + [\vartheta^T \psi_x - \lambda^T(t_f)]\, dx(t_f) +$$

$$[\lambda^T f_4 - \pi_3]\, dt_f + [-\pi_1 - \lambda_m(t_s^-)]\, dm(t_s^-) +$$

$$+ [\pi_1 + \lambda_m(t_s^+)]\, dm(t_s^+) + [-\pi_2 + \lambda^T(t_1^-) f_1 - \lambda^T(t_1^+) f_2]\, dt_1$$

$$+ [\pi_3 + \lambda^T(t_2^-) f_3 - \lambda^T(t_2^+) f_4]\, dt_2 - \lambda^T(t_1^-) dx(t_1^-)$$

$$+ \lambda^T(t_1^+) dx(t_1^+) + [\lambda^T(t_s^-) f_2 - \lambda^T(t_s^+) f_3]\, dt_s$$

$$- \lambda^T(t_2^-)\, dx\,(t_2^-) + \lambda^T(t_2^+)\, dx\,(t_2^+) \qquad \text{(C-9)}$$

$$+ \int_{t_o}^{t_1^-} [(\lambda^T f_{1_x} + \dot{\lambda}^T)\, \delta_x + f_{1_u}\, \delta u]\, dt$$

$$+ \int_{t_1^+}^{t_s^-} [(\lambda^T f_{2_x} + \dot{\lambda}^T)\, \delta_x + f_{2_u}\, \delta u]\, dt$$

$$+ \int_{t_s^+}^{t_2^-} [(\lambda^T f_{3_x} + \dot{\lambda}^T)\, \delta_x + f_{3_u}\, \delta u]\, dt$$

$$+ \int_{t_2^+}^{t_f} [(\lambda^T f_{4_x} + \dot{\lambda}^T)\, \delta_x + f_{4_u}\, \delta u]\, dt$$

Requiring each coefficient of the nonzero differentials in the states (dx) and times (dt) to be zero yield the necessary conditions.

Three classes of trajectories are examined in this thesis. They are:

Case One--only first stage fuel is completely used.

Case Two--only second stage fuel is completely used.

Case Three--both first and second stages are completely used. The necessary conditions will first be developed for each of the specific cases, followed by a listing of the conditions common to all three classes of trajectories.

Case One. The first case dictates that we are on the boundary of the first stage fuel constraint and inside the boundary region of the second stage constraint. Examination of the theory of constrained minimization (Ref 1) provides insight regarding the lagrange multipliers in Eq (C-7). Being on the first stage burn constraint indicates that π_2 is nonzero and being inside the second stage constraint gives π_3 the value of zero. Burning all of the first stage fuel also indicates that we are on the boundary of the mass constraint, giving π_1, a nonzero value. We also know that a complete burning of the first stage gives

$$dm(t_s^-) = dm(t_s^+) \tag{C-10}$$

since the structure drop-off weight is fixed. The resulting necessary conditions from Eq (C-9) peculiar to case one are therefore:

$$H_4(t_f) = 0$$

$$\lambda_m(t_s^-) = \lambda_m(t_s^+) = \pi_1 \qquad \text{(C-11)}$$

$$H_1(t_1^-) - H_2(t_1^+) = \pi_2$$

$$H_3(t_2^-) = H_4(t_2^+)$$

where $H_i = \lambda^T f_i$ *for* $i = 1, 4$

Case Two. For this class of trajectories we are inside the boundary region of the first stage burn constraint and have met the constraint for the second stage burning period. Constrained minimization theory dictates that π_1 and π_2 are zero and that π_3 is nonzero. Due to the fact that the first stage fuel may not be completely used,

$$dm(t_s^-) \neq dm(t_s^+) \qquad \text{(C-12)}$$

The necessary conditions unique to case two are:

$$H(t_f) = \pi_3$$

$$\lambda_m(t_s^-) = \lambda_m(t_s^+) = 0 \qquad \text{(C-13)}$$

$$H_1(t_1) = H_2(t_1)$$

$$H_4(t_2) - H_3(t_2) = \pi_3$$

Case Three. The third case indicates that we are on the boundary region for all three intermediate constraints. The associated lagrange multipliers are therefore all zero. The necessary

conditions become:

$$\lambda_m(t_s^-) = \lambda_m(t_s^+) = \pi_1$$

$$H_4(t_f) = \pi_3 \qquad \text{(C-14)}$$

$$H_1(t_1) - H_2(t_1) = \pi_2$$

$$H_3(t_2) - H_4(t_2) = -\pi_3$$

General Necessary Conditions. The necessary conditions that must be met for this problem in each of the three cases can be determined from the remaining terms in Eq (C-9). Those equations are:

$$\lambda_x(t) \text{ continuous for all } x \qquad \text{(C-15)}$$

$$H_2(t_s) = H_3(t_s) \qquad \text{(C-16)}$$

$$\phi_x = -\lambda^T(t_o) \rightarrow \lambda_m(t_o) = +1 \qquad \text{(C-17)}$$

$$\vartheta^T \psi_x = \lambda^T(t_f) \qquad \text{(C-18)}$$

$$\lambda_m(t_f) = 0 \qquad \text{(C-19)}$$

$$\dot{\lambda}^T = -\frac{\partial H}{\partial x} \qquad \text{(C-20)}$$

$$\frac{\partial H}{\partial u} = 0 \qquad \text{(C-21)}$$

The equations that correspond to Eq (C-18) are commonly referred to as the transversality conditions. Those equations corresponding to Eq (C-20) yield the costate equations and Eq (C-21) gives the optimality condition on the control.

Appendix D

Computer Listing of Coplanar Problem

```
      PROGRAM ORBTRAN(INPUT,OUTPUT,TAPE5=INPUT,TAPE6=OUTPUT)
C THIS PROGRAM WILL SOLVE THE MAXIMUM PAYLOAD COPLANAR ORBITAL TRANSFER
C PROBLEM FOR A TWO STAGE SOLID FUEL TUS.
      COMMON/MAIN/ PI,RFO,HFO,VRFO,RO,HO,   C1,C2,TH,THETAF,G,MU
      COMMON/CANON/DUFT,DUNM,TU,DUTUFT,DUTUNM,DU3TU2,CMU,CTU
      COMMON/MASS/ FM
      COMMON/TIME/ TF3,TS3
      DIMENSION Y(6),F(6),AJINV(6,6),W(180)
      REAL MU,ISP1,ISP2
      N=6
      PI=ACOS(-1.)
      MU=1.
C THE FOLLOWING DATA REPRESENTS THE CANONICAL UNITS USED TO NORMALIZE
C THE BOUNDARY VALUE PROBLEM
C         DISTANCE UNIT                 DU
C         TIME UNIT                     TU
C         VELOCITY UNIT                 DUTU
C         GRAVITATIONAL PARAMETER       DU3TU2
C         MASS UNIT                     CMU      (LB-SEC**2/FT)
C         THRUST UNIT                   CTU      (LBS)
      DUFT=2.092574E7
      TU=806.8136
      DUTUFT=2.59362854
      DU3TU2=1.407654216
      CMU=5000.
      CTU=(CMU*DUTUFT**2)/DUFT
C *****      INPUT PARAMETERS      *****
C "ISP1" IS THE SPECIFIC IMPULSE OF STAGE ONE MOTOR
C "ISP2" IS THE SPECIFIC IMPULSE OF STAGE TWO MOTOR
C "G" IS GRAVITY AT EARTH SURFACE
```

```
C "C1" IS EXHAUST VELOCITY OF STAGE ONE    MOTOR
C "C2" IS EXHAUST VELOCITY OF STAGE TWO MOTOR
C PO IS THE SEMI-LATUS RECTUM OF THE INITIAL PARKING ORBIT
C EO IS THE ECCENTRICITY OF THE INITIAL PARKING ORBIT
C PF IS THE SEMI-LATUS RECTUM OF THE TARGET ORBIT
C EF IS THE ECCENTRICITY OF THE TARGET ORBIT
C THETAF IS THE DESIRED ORBITAL TRANSFER ANGLE
C "RFD" IS THE DESIRED FINAL RADIUS
C "HFD" IS THE DESIRED FINAL ANGULAR MOMENTUM
C "VRFD" IS THE DESIRED FINAL RADIAL VELOCITY
C TFB IS THE TIME FOR FIRST STAGE BURNING
C TSB IS THE TIME FOR SECOND STAGE BURNING
      ISP1=291.3
      ISP2=300.3
      G=32.2
      C1=ISP1*G/OUTUFT
      C2=ISP2*G/OUTUFT
      READ *, PO,EO,PF,EF,THETAF
      PRINT *,  "PO,EO,PF,EF ....."
      PRINT *, PO,EO,PF,EF
      READ *, TFB,TSB
      PO=PO*6076.115+OUFT
      PF=PF*6076.115+OUFT
      THETAF=THETAF*PI/180
      ICOUNT=0
      ICOUNT=ICOUNT+1
      RFD=PF/(1+EF*COS(THETAF))
      HFD=SQRT(PF*DU3TU2)
      VRFD=EF*HFD*SIN(THETAF)/PF
      PO=PO/(1+EO)
```

```
      H0=SQRT(R0*DU3TU2)
C THE Y VECTOR REPRESENTS THE UNKNOWN QUANTITIES VARIED BY NS01A
C TO YIELD SOLUTIONS TO THE BOUNDARY VALUE PROBLEM.
C         Y(1) = LAMBDA R.
C         Y(2) = LAMBDA THETA
C         Y(3) = LAMBDA VR.
C         Y(4) = LAMBDA H.
C         Y(5) = MASS AT T0.
C         Y(6) = : IGNITION OF SECOND STAGE
      IF (ICOUNT .GT. 1) GO TO 10
      READ *, Y
C THE INPUT PARAMETERS REQUIRED BY NS01A ARE ...
      READ *, DMAX,MAXFUN,ACC,DSTEP,IPRINT
   10 CONTINUE
      Y(5)=Y(5)/10
      Y(6)=Y(6)/100
      CALL NS01A(N,Y,F,AJINV,DSTEP,DMAX,ACC,MAXFUN,IPRINT,W)
      ICOUNT=ICOUNT+1
      ANGLE=THETAF*180/PI
      PRINT *, "THETAF = " ,ANGLE
      Y(5)=Y(5)*10
      Y(6)=Y(6)*100
      PRINT *, Y
      FM=FM*5001*32.2
      PRINT *, "  MASS AT FINAL TIME IS .....", FM
      TOMA=Y(5)*5000*32.2
      PRINT *, " INITIAL MASS ..... " , TOMA
      PRINT *, " FIRST BURN IS "  ,TFB
      PRINT *, "  SECOND BURN IS "    ,TSB
      END
```

AD-A034 947 AIR FORCE INST OF TECH WRIGHT-PATTERSON AFB OHIO SCH--ETC F/G 22/2
MAXIMUM PAYLOAD ORBITAL TRANSFERS FOR A SPACE SHUTTLE SOLID-FUE--ETC(U)
DEC 76 J W MOCKO

UNCLASSIFIED GA/MC/76D-11 NL

2 OF 2
ADA034947

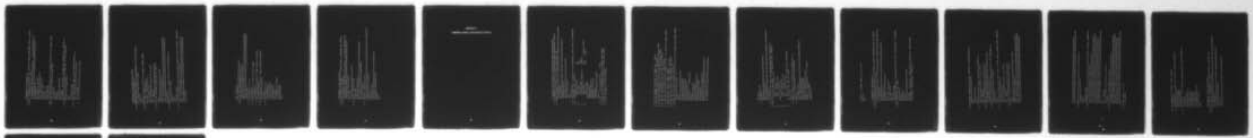

END

DATE
FILMED
3-77

```
      SUBROUTINE CALFUN(N,Y,F)
C THIS SUBROUTINE PROVIDES THE TERMINAL ERROR FUNCTIONS USED BY NS01A
C AFTER INTEGRATION OF THE MPBVP
      COMMON/MAIN/ PI,RED,HED,VRED,RO,HO,   C1,C2,TH,THETAF,C,MU
      COMMON/CANON/DUFT,DUNM,TU,DUTUFT,DUTUNM,DU3TU2,CMU,CTU
      COMMON/MASS/ EM
      COMMON/TIME/ TFR,TSR
      DIMENSION Y(6),F(6),X(10)
      REAL LNTF,MU,KT1,KT2
      EXTERNAL SLOPE
      NIS=312
      Y(5)=Y(5)*10
      Y(6)=Y(6)*100
C THE INITIAL CONDITIONS FOR THE FIRST SECTION OF THE MPBVP FROM
C "TO" TO "T1-" ARE NORMALIZED AND ARE:
      X(1)=RO/DUFT
      X(2)=0.
      X(3)=0.
      X(4)=HO*TU/(DUFT**2)
      X(5)=Y(5)
      X(6)=Y(1)   $X(7)=Y(2)   $X(8)=Y(3)   $X(9)=Y(4)   $X(10)= 1.
C QUANTITIES REQUIRED FOR FIRST PORTION OF INTEGRATION:
      DT=(TFR/TU)/FLOAT(NIS)
      T=0
      C=C1
      TH=41767.4/CTU
C INTEGRATION ROUTINE UNTIL FIRST STAGE CUTOFF....
      CALL SET(10,T,X,DT,SLOPE,0,.T.,0,D)
      DO 1 J=1,NIS
    1 CALL STEP(10,T,X,DT,SLOPE,0,.T.,0,D)
```

```
      P=SQRT(X(3)**2+X(9)**2*X(1)**2)
      KT1=-1*(P/X(5)+X(10)/C)
C QUANTITIES REQUIRED FOR SECOND PORTION OF INTEGRATION....
      DT= (X(6)-TSB/TU)/FLOAT(NIS)
      T=TSB/TU
      TH=0
C INTEGRATION ROUTINE FROM FIRST STAGE CUTOFF UNTIL
C SECOND STAGE IGNITION....
      DELTAM = 2437./32.2/3MU
      X(5)=X(5)-DELTA1
      CALL SET(10,T,X,DT,SLOPE,D,.T.,0,0)
      DO 2 J=1,NIS
    2 CALL STEP(10,T,X,DT,SLOPE,D,.T.,0,0)
C KT2 IS THE SWITCHING FUNCTION AT TIME T2
      C=C2
      P=SQRT(X(8)**2+X(9)**2*Y(1)**2)
      KT2=-1.*(P/X(5)+X(10)/C)
      H3T2  =X(5)*X(3)+X(7)*X(4)/(X(1)**2)+X(8)*(X(4)**2/(X(1)**3)
     .-MU/(X(1)**2)-TH*X(8)/(P*X(5)))-X(9)**2*X(1)**2*TH/(P*X(5))
     .-X(10)*TH/C
C QUANTITIES FOR THE THIRD PORTION OF INTEGRATION...
      DT=TSB/TU/FLOAT(NIS)
      T=Y(6)
      C=C2
      TH=14076.6/CTU
C INTEGRATION ROUTINE FROM SECOND STAGE IGNITION UNTIL ORBITAL TRANSFER.
      CALL SET(10,T,X,DT,SLOPE,D,.T.,0,0)
      H4T2  =X(5)*X(3)+X(7)*X(4)/(X(1)**2)+X(8)*(X(4)**2/(X(1)**3)
     .-MU/(X(1)**2)-TH*X(8)/(P*X(5)))-X(8)**2*X(1)**2*TH/(P*X(5))
     .-X(10)*TH/C
```

```
      DO 3 J=1,NIS
    3 CALL STEP(10,T,X,DT,SLOPE,D,.T.,D,D)
C HAMTF IS THE HAMILTONIAN AT TIME TF
      P=SQRT(X(8)**2+X(9)**2*X(1)**2)
      HAMTF =X(6)*X(3)+X(7)*X(4)/(X(1)**2)+X(8)*(X(4)**2/(X(1)**3)
     .-MU/(X(1)**2)-TH*X(8)/(P*X(5)))-X(9)**2*X(1)**2*TH/(P*X(5))
     .-X(10)*TH/C
C LMTF IS LAMBDA 4 AT TF
      LMTF=X(10)
C RFN IS NORMALIZED DESIRED FINAL RADIUS
      RFN=RFD/DUFT
C VRFN IS NORMALIZED DESIRED FINAL RADIAL VELOCITY
      VRFN=VRFD/DUTUFT
C HFN IS NORMALIZED DESIRED FINAL ANGULAR MOMENTUM
      HFN=HFD*TU/(DUFT**2)
      FM=X(5)
C ERROR FUNCTIONS ARE
      F(1)=RFN-X(1)
      F(2)=THETAF-X(2)
      F(3)=VRFN-X(3)
      F(4)=HFN-X(4)
      F(5)=LMTF
      F(6)=HAMTF+H3T2-H4T2
      Y(5)=Y(5)/10
      Y(6)=Y(6)/100
      END
```

```
      SUBROUTINE SLOPE(N,T,X,DX)
C THIS SUBROUTINE CONTAINS THE DIFFERENTIAL EQUATIONS OF MOTION
C FOR THE COPLANAR PROBLEM.
      COMMON/MAIN/ PI,RED,HED,VRED,RO,HO,    C1,C2,TH,THETAF,C,MU
      COMMON/CANON/DUET,DUNM,TU,DUTUET,DUTUNM,DU3TU2,CMU,CTU
      DIMENSION X(10),DX(10)
      REAL MU
      P= SQRT(X(8)**2+X(9)**2*X(1)**2)
C THE STATE EQUATIONS ARE
      DX(1)=X(3)
      DX(2)=X(4)/(X(1)**2)
      DX(3)=X(4)**2/(X(1)**3)-MU/(X(1)**2)-TH*X(8)/(P*X(5))
      DX(4)=-1.*TH*X(1)**2*X(9)/(X(5)*P)
      DX(5)=-1.*TH/C
C THE COSTATE EQUATIONS ARE:
      DX(6)=1./(X(1)**3)*(2.*X(7)*X(4)+3.*X(8)*X(4)**2/X(1)-2.*X(8)*MU)
     .+X(9)**2*X(1)*TH/(X(5)*P)
      DX(7)=0.
      DX(8)=-1.*X(6)
      DX(9)=-1./(X(1)**3)*(X(7)*X(1)+2.*X(8)*X(4))
      DX(10)=-1.*TH*P/(X(5)**2)
      RETURN
      END
```

Appendix E

Computer Listing of Noncoplanar Problem

```
      PROGRAM ORBTRAN(INPUT,OUTPUT,TAPE5=INPUT,TAPE6=OUTPUT)
C THIS PROGRAM WILL SOLVE THE MAXIMUM PAYLOAD NONCOPLANAR ORBITAL
C TRANSFER PROBLEM FOR A TWO STAGE SOLID FUEL IUS
      COMMON/MAIN/PI,RFD,THETAFD,PHIFD,VRFD,VTFD,VPFD,TH,C1,C2,C,RD,HO,
     ,P, ANGINC,MU
      COMMON/CANON/DUFT,DUNM,TU,DUTUFT,DUTUNM,DU3TU2,CMU,CTU
      COMMON/MASS/ FM
      DIMENSION Y(8),F(8),AJINV(8,8),W(250)
      REAL MU,ISP1,ISP2
      N=8
      PI=ACOS(-1.)
C THE FOLLOWING DATA REPRESENTS THE CANONICAL UNITS USED TO NORMALIZE
C THE BOUNDARY VALUE PROBLEM
C        DISTANCE UNIT                  DU
C        TIME UNIT                      TU
C        VELOCITY UNIT                  DUTJ
C        GRAVITATIONAL PARAMETER        DU3TU2
C        MASS UNIT                      CMJ      (LB-SEC**2/FT)
C        THRUST UNIT                    CTU      (LBS)
      DUFT=2.0925745E7
      TU=806.8136
      DUTUFT=2.59362854
      DU3TU2=1.407654716
      CMU=5000.
      CTU=(CMU*DUTUFT**2)/DUFT
      MU=1.
C *****      INPUT PARAMETERS      *****
C "ISP1" IS THE SPECIFIC IMPULSE OF STAGE ONE MOTOR
C "ISP2" IS THE SPECIFIC IMPULSE OF STAGE TWO MOTOR
C "G" IS GRAVITY AT EARTH SURFACE
```

```
C "C1" IS EXHAUST VELOCITY OF STAGE ONE    MOTOR
C "C2" IS EXHAUST VELOCITY OF STAGE TWO MOTOR
C PO IS THE SEMI-LATUS RECTUM OF THE INITIAL PARKING ORBIT
C EO IS THE ECCENTRICITY OF THE INITAAL PARKING ORBIT
C PF IS THE SEMI-LATUS RECTUM OF THE TARGET ORBIT
C EF IS THE ECCENTRICITY OF THE TARGET ORBIT
C THETAF IF THE DESIRED ORBITAL TRANSFER ANGLE IN PLANE OF FINAL ORBIT
C "RFD" IS THE DESIRED FINAL RADIUS
C "HFD" IS THE DESIRED FINAL ANGULAR MOMENTUM
C "VRFD" IS THE DESIRED FINAL RADIAL VELOCITY
C "C" IS THE EFFECTIVE EXHAUST VELOCITY
C ANGINC IS THE ANGLE OF INCLINATION BETWEEN THE INITIAL AND FINAL ORBIT
      PO=150.*6076.115+DUFT
      EO=0.
      READ *, PF,EF,THETAF,ANGINC
      ANGINC=ANGINC*PI/180
      THETAF=THETAF*PI/180
      PF=PF*6076.115+DUFT
      ICOUNT=ICOUNT+1
      ISP1=281.8      *ISP2=300.8
      G=32.2
      C1=ISP1*G/DUTUFT
      C2=ISP2*G/DUTUFT
      RFD=PF/(1+EF*COS(THETAF))
      HFD=SQRT(PF*DU3TU2)
      RO=PO/(1+EO)
      VRFD=EF*HFD*SIN(THETAF)/PF
      PHIFD=ASIN(-1.*COS(THETAF)*SIN(ANGINC))
      IF (ANGINC .EQ. 0) GO TO 2
      THETAFD=ACOS(-1.*TAN(PHIFD)/TAN(ANGINC))
```

```
      GO TO 3
    2 THETAFD=THETAF
    3 CONTINUE
      VRFD=-1.*HFD*SIN(ANGINC)*SIN(THETAFD)/RFD
      PHIFD=PI/2-PHIFD
      VTFD=(HFD/RFD)*(COS(ANGINC)-SIN(ANGINC)*COS(THETAFD)*COS(PHIFD)/
     .SIN(PHIFD))
C THE Y VECTOR REPRESENTS THE UNKNOWN QUANTITIES VARIED BY
C NSO1A TO YIELD SOLUTIONS TO THE BOUNDARY VALUE PROBLEM
C        Y(1) = MASS AT TIME TO
C        Y(2) = LAMBDA R
C        Y(3) = LAMBDA THETA
C     Y(4) = LAMBDA PHI
C        Y(5) = LAMBDA VR
C        Y(6) = LAMBDA V THETA
C        Y(7) = LAMBDA V PHI
C        Y(8) = "T2  TIME AT SECOND STAGE IGNITION"
      IF (ICOUNT .GT. 1) GO TO 10
      READ *, Y
C THE INPUT PARAMETERS REQUIRED BY NSO1A ARE ...
      READ *, DMAX,MAXFUN,ACC,DSTEP,IPRINT
   10 CONTINUE
      Y(8)=Y(8)/1000
      CALL NSO1A(N,Y,F,AJINV,DSTEP,DMAX,ACC,MAXFUN,IPRINT,W)
      ANGLE=THETAF*180/PI
      ANGLE1=ANGINC*180/PI
      PRINT *, "THETAF = ", ANGLE
      PRINT *, "INCLINATION =   ", ANGLE1
      Y(8)=Y(8)*1000
      PRINT *, Y
```

```
      PRINT *, " FINAL MASS IS ....", FM
      GO TO 1
      END



      SUBROUTINE CALFUN(N,Y,F)
C THIS SUBROUTINE PROVIDES THE TERMINAL ERROR FUNCTIONS USED BY NSOLA
C AFTER INTEGRATION OF THE MPBVP
      COMMON/MAIN/PI,RFD,THETAFD,PHIFD,VRFD,VTFD,VPFD,TH,C1,C2,C,RO,HO,
     *P, ANGINC,MU
      COMMON/CANON/DUFT,DUNM,TU,DUTUFT,DJTUNM,DU3TU2,CMU,CTJ
      COMMON/MASS/ FM
      DIMENSION Y(8),X(14),F(8)
      REAL MU
      REAL LMTF,KT1,KT2,P
      EXTERNAL SLOPE
      NIS=512
      Y(8)=Y(8)*1000
C THE NORMALIZED INITIAL CONDITIONS FOR THE FIRST SECTION OF THE MPBVP
C FROM "TO" TO "T1-" ARE:
      X(1)=RO/DUFT
      X(2)=0.
      X(3)=PI/2.
      X(4)=0.
      X(5)=(SQRT(DU3TU2/RO))/DUTUFT
      X(6)=0.
      X(7)=Y(1)   $X(8)=Y(2)   $X(9)=Y(3)  $X(10)=Y(4)   $X(11)=Y(5)
      X(12)=Y(6)   $X(13)=Y(7)   $X(14)= 1.
```

```
C QUANTITIES REQUIRED FOR FIRST PORTION OF INTEGRATION....
      DT=(139.52/TU)/FLOAT(NIS)
      T=0
      TH=41757.4/CTU
      C=C1
C INTEGRATION ROUTINE UNTIL FIRST STAGE CUTOFF....
      CALL SET(14,T,X,DT,SLOPE,D,.T.,D,D)
      DO 1 J=1,NIS
    1 CALL STEP(14,T,X,DT,SLOPE,D,.T.,D,D)
C KT1 IS THE SWITCHING FUNCTION AT TIME T1
      P=SQRT(X(11)**2+(X(12)/SIN(X(3)))**2+X(13)**2)
      KT1=-1.*(P/X(7)+X(14)/C)
C QUANTITIES REQUIRED FOR SECOND PORTION OF INTEGRATION....
      DT=(X(8)-139.52/TU)/FLOAT(NIS)
      T=139.52/TU
      TH=0
C INTEGRATION ROUTINE FROM FIRST STAGE CUTOFF UNTIL SECOND STAGE IGNITIO
      DELTAM=(2437./32.2)/CMU
      X(7)=X(7)-DELTAM
      CALL SET(14,T,X,DT,SLOPE,D,.T.,D,D)
      DO 2 J=1,NIS
    2 CALL STEP(14,T,X,DT,SLOPE,D,.T.,D,D)
C KT2 IS THE SWITCHING FUNCTION AT TIME T2
      C=C2
      P=SQRT(X(11)**2+(X(12)/SIN(X(3)))**2+X(13)**2)
      KT2=-1.*(P/X(7)+X(14)/C)
      H3T2 =X(8)*X(4)+X(9)*X(5)/X(1)+X(10)*X(6)/X(1)+X(11)*(X(5)**2/
     .X(1)+(X(5)**2*SIN(X(3))**2)/X(1)-MJ/(X(1)**2)-TH*X(11)/(X(7)*P))
     .+X(12)*(-1.*X(4)*X(5)/X(1)-2.*X(5)*X(6)*COS(X(3))/(SIN(X(3))
```

```
     .*X(1))-TH*X(12)/(X(7)*SIN(X(3))**2*P))+X(13)*(-1.*X(4)*X(6)/
     .X(1)+X(5)**2*SIN(X(3))*COS(X(3))/X(1)-TH*X(13)/(X(7)*P))-X(14)*TH/
     .C
C QUANTITIES FOR THE THIRD PORTION OF INTEGRATION....
      DT=100.4/TU/FLOAT(NIS)
      T=Y(8)
      C=C2
      TH=14076.6/CTU
C INTEGRATION ROUTINE FROM SECOND STAGE IGNITION UNTIL ORBITAL TRANSFER.
      CALL SET(14,T,X,DT,SLOPE,0,.T.,0,0)
      P=SQRT(X(11)**2+(X(12)/SIN(X(3)))**2+X(13)**2)
      H4T2 =X(8)*X(4)+X(9)*X(5)/X(1)+X(10)*X(6)/X(1)+X(11)*(X(5)**2/
     .X(1)+(X(5)**2*SIN(X(3))**2)/X(1)-MU/(X(1)**2)-TH*X(11)/(X(7)*P))
     .+X(12)*(-1.*X(4)*X(5)/X(1)-2.*X(5)*X(6)*COS(X(3))/(SIN(X(3))
     .*X(1))-TH*X(12)/(X(7)*SIN(X(3))**2*P))+X(13)*(-1.*X(4)*X(6)/
     .X(1)+X(5)**2*SIN(X(3))*COS(X(3))/X(1)-TH*X(13)/(X(7)*P))-X(14)*TH/
     .C
      DO 3 J=1,NIS
    3 CALL STEP(14,T,X,DT,SLOPE,0,.T.,0,J)
      FM=X(7)
C HAMTF IF THE HAMILTONIAN AT TIME TF
      P=SQRT(X(11)**2+(X(12)/SIN(X(3)))**2+X(13)**2)
      HAMTF=X(8)*X(4)+X(9)*X(5)/X(1)+X(10)*X(6)/X(1)+X(11)*(X(5)**2/
     .X(1)+(X(5)**2*SIN(X(3))**2)/X(1)-MU/(X(1)**2)-TH*X(11)/(X(7)*P))
     .+X(12)*(-1.*X(4)*X(5)/X(1)-2.*X(5)*X(6)*COS(X(3))/(SIN(X(3))
     .*X(1))-TH*X(12)/(X(7)*SIN(X(3))**2*P))+X(13)*(-1.*X(4)*X(6)/
     .X(1)+X(5)**2*SIN(X(3))*COS(X(3))/X(1)-TH*X(13)/(X(7)*P))-X(14)*TH/
     .C
C LMTF IF LAMBDA M AT TF
      LMTF=X(14)
```

```
C RFN IS NORMALIZED DESIRED FINAL RADIUS
      RFN=RFD/DUFT
C VRFN,VTFN,VPFN ARE NORMALIZED DESIRED FINAL VELOCITIES
      VRFN=VRFD/DUTUFT
      VTFN=VTFD/DUTUFT
      VPFN=VPFD/DUTUFT
C "F" REPRESENTS ERROR FUNCTION WHICH NSOLA BRINGS WITHIN ACC
      F(1)=LMTF
      F(2)=RFN-X(1)
      F(3)=THETAFD-X(2)
      F(4)=PHIFD-X(3)
      F(5)=VRFN-X(4)
      F(6)=VTFN-X(5)
      F(7)=VPFN-X(6)
      F(8)=HAMTF+H3T2-H+T2
      Y(8)=Y(8)/1000
      END


      SUBROUTINE SLOPE (N,T,X,DX)
C THIS SUBROUTINE CONTAINS THE DIFFERENTIAL EQUATIONS OF
C MOTION FOR THE NONCOPLANAR PROBLEM
      COMMON/MAIN/PI,RFD,THETAFD,PHIFD,VRFD,VTFD,VPFD,TH,C1,C2,C,RO,HO,
     *P, ANGINC,MU
      COMMON/CANON/DUFT,DUNM,TU,DUTUFT,DJTUNM,DU3TU2,CMU,CTU
      DIMENSION X(14),DX(14)
      REAL MU
      R=SQRT(X(11)**2+(X(12)/SIN(X(3)))**2+X(13)**2)
```

```
      DX(1)=X(4)
      DX(2)=X(5)/X(1)
      DX(3)=X(5)/X(1)
      DX(4)=(X(5)**2)/X(1)+(X(5)**2*SIN(X(3))**2)/X(1)-MU/(X(1)**2)
     .-(TH*X(11))/(P*X(7))
      DX(5)=(-1./X(1))*(X(4)*X(5)+(2.*X(5)*X(5)*COS(X(3)))/SIN(X(3)))
     .-(TH*X(12))/(P*SIN(X(7))**2*X(7))
      DX(6)=(-1./X(1))*(X(4)*X(6)-X(5)**2*SIN(X(3))*COS(X(3)))-TH*X(13)/
     .(P*X(7))
      DX(7)=-1.*TH/C
      DX(8)=1./(X(1)**2)*(X(9)*X(5)+X(10)*X(6)+X(11)*(X(5)**2+X(5)**2*
     .SIN(X(3))**2-(2.*MU)/X(1))-X(12)*(X(4)*X(5)+(2.*X(5)*X(6)*COS(X(3)
     .)/SIN(X(3)))-X(13)*(X(4)*X(6)-X(5)**2*SIN(X(3))*COS(X(3))))
      DX(9)=0.0
      DX(10)=(-1./X(1))*(2.*X(11)*X(5)**2*SIN(X(3))*COS(X(3))+(2.*X(12)
     .*X(5)*X(6))/(SIN(X(3))**2)+(X(13)*X(5)**2)*(COS(X(3))**2-SIN(X(3))
     .**2))-(X(12)**2*TH*COS(X(3)))/(P*SIN(X(3))**3*X(7))
      DX(11)=1./X(1)*(X(12)*X(5)+X(13)*X(6))-X(8)
      DX(12)=-1./X(1)*(X(9)+2.*X(11)*X(5)*SIN(X(3))**2-X(12)*X(4)
     .-(2.*X(6)*X(12)*COS(X(3)))/SIN(X(3))+2.*X(13)*X(5)*SIN(X(3))*COS(X
     .(3)))
      DX(13)=1./X(1)*(-1.*X(10)-2.*X(11)*X(6)+2.*X(12)*X(5)*COS(X(3))/
     .SIN(X(3))+X(13)*X(4))
      DX(14)=-1.*TH*P/(X(7)**2)
      RETURN
      END
```

Vita

John W. Mocko was born 19 November 1949 in Little Falls, New York. He graduated from Little Falls High School in 1967. After spending a year at the U.S. Air Force Academy Preparatory School he entered the Air Force Academy in June 1968. He earned a Bachelor of Science Degree in Basic Sciences in June 1972, but was not commissioned due to medical disqualifications.

In September 1972, he began teaching high school science and coaching football, basketball and track. After two years of teaching he was granted a waiver for his commission by the Secretary of the Air Force in August 1974. His first assignment was at the Occupational Measurement Center at Lackland AFB, Texas as a test psychologist. He remained there until he entered the AFIT School of Engineering in June 1975.

UNCLASSIFIED

SECURITY CLASSIFICATION OF THIS PAGE *(When Data Entered)*

REPORT DOCUMENTATION PAGE		READ INSTRUCTIONS BEFORE COMPLETING FORM
1. REPORT NUMBER GA/MC/76D-11	2. GOVT ACCESSION NO.	3. RECIPIENT'S CATALOG NUMBER
4. TITLE *(and Subtitle)* MAXIMUM PAYLOAD ORBITAL TRANSFERS FOR A SPACE SHUTTLE SOLID-FUEL UPPER STAGE VEHICLE		5. TYPE OF REPORT & PERIOD COVERED MS Thesis 6. PERFORMING ORG. REPORT NUMBER
7. AUTHOR(s) John W. Mocko 1 LT, USAF		8. CONTRACT OR GRANT NUMBER(s)
9. PERFORMING ORGANIZATION NAME AND ADDRESS Air Force Institute of Technology (AFIT/EN) Wright-Patterson AFB, Ohio 45433		10. PROGRAM ELEMENT, PROJECT, TASK AREA & WORK UNIT NUMBERS
11. CONTROLLING OFFICE NAME AND ADDRESS		12. REPORT DATE December 1976 13. NUMBER OF PAGES 111
14. MONITORING AGENCY NAME & ADDRESS*(if different from Controlling Office)*		15. SECURITY CLASS. *(of this report)* UNCLASSIFIED 15a. DECLASSIFICATION/DOWNGRADING SCHEDULE

16. DISTRIBUTION STATEMENT *(of this Report)*

Approved for public release; distribution unlimited

17. DISTRIBUTION STATEMENT *(of the abstract entered in Block 20, if different from Report)*

18. SUPPLEMENTARY NOTES

Approved for public release; IAW AFR 190-17

JERRAL F. GUESS, Captain, USAF
Director of Information

19. KEY WORDS *(Continue on reverse side if necessary and identify by block number)*

Upper Stage Vehicle	Energy Management	Orbital Transfers
Interim Upper Stage	Thrust Termination	Space Shuttle
Maximum Payload	Offloading Fuel	
Optimization	Sizing Analysis	

20. ABSTRACT *(Continue on reverse side if necessary and identify by block number)*

A two-stage, solid-fuel proposal for the Interim Upper Stage Vehicle of the Space Transportation System has been selected for use by the Department of Defense. It is the purpose of this study to investigate the capabilities of such a vehicle in terms of the maximum payload which can be delivered to orbit. This optimal payload problem is examined in light of three energy management

over

DD FORM 1 JAN 73 1473 EDITION OF 1 NOV 65 IS OBSOLETE

UNCLASSIFIED

SECURITY CLASSIFICATION OF THIS PAGE *(When Data Entered)*

techniques. The first technique, thrust termination, involves shutting off engine thrust prior to complete use of propellant. The second technique investigates the effects on payload of varying the central angle through which the transfer is made. The third technique, offloading, examines the possibility of reducing the amount of available fuel for either stage prior to the mission to determine if payloads can be increased. Finite burn periods are assumed in this study. A multipoint boundary value problem results from the appearance of interior constraints in the problem. A numerical technique is used to generate solutions for a range of transfers in the special coplanar problem. Conclusions are discussed for each of the three energy management techniques in the coplanar transfer. Even though non-optimal noncoplanar results were obtained it is believed that the general coplanar results can be extended to the noncoplanar problem.